

Mad1 and c-Myc interactions during peripheral axonal regeneration

by

Trevor Poitras

A thesis submitted in partial fulfillment of the requirements for the degree of

Master of Science

Neuroscience

University of Alberta

©Trevor Poitras, 2018

Abstract

The peripheral nervous system (PNS) is often damaged by physical trauma or by diseases known as neuropathies. Currently, there are no effective treatments for augmenting repair of damaged nerves. Although the PNS is considered to be more plastic than the central nervous system, recovery outcomes in patients with neuropathy or physical damage are often poor. Molecular approaches have been investigated as a way to ramp up the regeneration response following damage. The list of proteins within peripheral neurons that restrict regrowth of axons is growing, with proteins such as PTEN, RB1, and RhoA as members of this list¹⁻⁴.

A thorough understanding of the mechanisms regulating axon regeneration will allow for the development of molecular approaches that can be applied within a clinical setting. Here we investigate the role of Mad1 and c-Myc in models of regeneration. c-Myc is a prominent transcription factor that is oncogenically activated in a wide variety of cancers. Under normal circumstances, it functions to cause the growth and proliferation of cells, but can be utilized by cancers cells to promote tumorigenesis. In order to execute c-Myc's transcriptional functions, it must dimerize with Myc associated factor X (Max). This association can be inhibited by Mad1 to promote quiescence and differentiation of cells. We hypothesize that by inhibiting Mad1, there will be enhanced axonal regrowth through reduced competitive inhibition of Myc.

We first identified that these important mediators are found within the PNS. In this thesis, through the use of small interfering RNA (siRNA), we investigated the role that Mad1 and c-Myc play within the regeneration response. We show that knockdown

of Mad1 in dorsal root ganglion (DRG) cell cultures was sufficient to cause improvements in neurite extension. We also found that *in vivo* Mad1 knockdown within our sciatic crush injury model corresponded to improvements in functional recovery through behavioral and electrophysiological testing.

Additionally, we found that knocking down c-Myc with siRNA in cultured DRG neurons had no effect on the ability of these neurons to grow projections. However, we did find a substantial growth reduction in our cultures treated with 10058-F4, a small molecule that inhibits N- and c-Myc's association with Max.

Taken together these findings suggest an important role for the Myc/Max/Mad1 network within the peripheral nervous system. The growth-promoting effects associated with Mad1 inhibition presents an intervention node that may potentially lead to novel therapeutic applications.

Preface

This research was conducted at the University of Alberta under the supervision of Dr. Douglas Zochodne. Animal models of regeneration were used through the course of these experiments and Ethics approval was granted for these experiments by the University of Alberta Health Sciences Laboratory Animal Services (HSLAS). This thesis was written entirely by myself, with the exception of edits provided by my supervisory committee.

Acknowledgments

I would firstly like to thank my supervisor Dr. Douglas Zochodne for his constant support throughout my time in the lab. He has been a terrific mentor and has allowed me to grow and thrive as a scientist. I couldn't imagine having another supervisor who would have taught and challenged me in the same way Dr. Zochodne has. Thank you to all the members of the Zochodne Lab, Matt Larouche, Anand Krishnan, Prashanth Komirishetty, Arul Duraikannu, Twinkle Joy, Liam McCoy, Kasia Zubkow, and Ambika Chandrasekhar for providing constant moral and technical support throughout my time within the Lab. I would like to specifically thank Ambika for her help with the PCR for my experiments. I could not have finished my thesis without your help.

I would also like to thank Drs. Christine Webber and Peter Smith for their support and help in developing my experimental design. Additionally, I would like to thank Dr. Webber and Haecy Macandili for their help looking at Schwann cell proliferation as an extension of this thesis. Although further experiments will be necessary, I really appreciate the interest and help with this aspect of my project.

To all of you, I thank you and couldn't have made it this far without you.

Table of Contents

Abstract	ii
Preface	iv
Acknowledgments	v
List of figures.....	viii
Glossary of terms and abbreviations.....	ix
1. Introduction	1
2. Background	6
2.1 Peripheral nerve regeneration.....	6
2.2 Myc	11
2.2-1 Myc structure and function	11
2.2-2 -Myc and apoptosis	14
2.2-3 Other c-Myc interacting proteins	16
2.2 Mad1	19
2.3 Max	20
3. Methods.....	22
3.1 Animal models	22
3.2 RNA isolation and qRT-PCR	22
3.3 Adult sensory neuron cultures	23
3.4 Lesioning experiment	24
3.5 Neurite outgrowth assay.....	24
3.7 Electrophysiology.....	25
3.8 Hargreaves Behavioral Measurements.....	26
3.9 Von Frey Measurements	26
3.10 Western Blot.....	26
3.11 Immunohistochemistry	27
3.12 In vivo delivery of siRNA and electroporation	28

4. Results	29
4.1 Expression data	29
4.1-1 <i>c-Myc</i> expression in injured and uninjured DRGs.....	29
4.1-2 Max expression within injured and uninjured DRGs	31
4.1-3 <i>Mad1</i> expression within injured and uninjured DRGs	32
4.4 <i>Mad1</i> expression within the nucleolus of neurons	34
4.2 Knockdown of <i>Mad1</i> and <i>c-Myc</i> <i>in vitro</i>	35
4.3 <i>c-Myc</i> and <i>Mad1</i> knockdown and neurite outgrowth	37
4.3-1 <i>Mad1</i> Knockdown improves neurite outgrowth.....	37
4.3-2 <i>Mad1</i> knockdown does not cause apoptosis in cultured DRG neurons	39
4.3-3 <i>c-Myc</i> Knockdown has no effect on neurite outgrowth	40
4.4 N-Myc expression, 10058-F4 and neurite outgrowth	41
4.4-1 N-Myc expression in injured and uninjured DRGs	41
4.4-2 10058-F4 treated cultures decreases neurite outgrowth	42
4.5 <i>Mad1</i> siRNA <i>in vivo</i> experiments	44
5. Discussion	47
Conclusion	58
References	59

List of figures

Figure 1: STRING analysis of c-Myc and interacting partners	16
Figure 2: Molecular diagram of Myc interacting proteins	18
Figure 3: c-Myc protein and RNA expression in the DRG	30
Figure 4: Max protein and RNA expression in the DRG	31
Figure 5: Mad1 protein and RNA expression in the DRG	33
Figure 6: Mad1 expression within the nucleolus	35
Figure 7: Knockdown of Mad1 and c-Myc <i>in vitro</i>	36
Figure 8: Neurite outgrowth of DRG neurons following Mad1 knockdown	38
Figure 9: TUNEL Staining of DRGs following Mad1 knockdown	39
Figure 10: Neurite outgrowth of DRG neurons followin c-Myc knockdown.....	40
Figure 11: N-Myc RNA expression within the DRG	42
Figure 12: Neurite outgrowth of neurons treated with 10058-F4	43
Figure 13: <i>in vivo</i> treatment of Mad1 siRNA following sciatic crush.....	46

Glossary of terms and abbreviations

Akt: Protein Kinase B

Avian Myelocytomatosis viral oncogene homologue: c-Myc

Avian Myelocytomatosis viral oncogene neuroblastoma derived homologue: N-Myc

Central nervous system: CNS

CGRP: Calcitonin gene-related peptide

CMAP: Compound motor action potential

Cyclin dependent kinase: CDK

Dorsal root ganglion: DRG

E2F: E2 factor

EMT: Epithelial mesenchymal transition

GFAP: Glial fibrillary acidic protein

Glycogen synthase kinase 3 β : GSK3 β

Max dimerization protein: Mad1

Mitogen activated protein kinase: ERK1/2 (MAPK)

Myc associated factor X: Max

Nerve growth factor: NGF

P75: Low affinity NGF receptor

Perikarya: Neuronal cell bodies

Peripheral nervous system: PNS

phosphatase and tensin homolog deleted on chromosome 10: PTEN

PI3K: Phosphoinositide 3-kinase

PSC: Pluripotent stem cell.

Retinoblastoma1: RB1

Schwann cells: SC

Small interfering ribonucleic acids: siRNA

SNAP: Sensory nerve action potential

Unc5H2: Netrin receptor

1. Introduction

The peripheral nervous system (PNS) is often damaged from physical trauma or through disruption caused by diseases. Nerves with damage are known as neuropathies. For example, with the rising prevalence of diabetes, there is a concurrent increase in the number of diabetic patients experiencing neuropathy. There are no approved effective treatments for improving the regeneration of the human peripheral nervous system, and this has functional consequences for patients. Following axotomy, only 10% of axons are able to cross the injury site and reinnervate their targets⁵. This can manifest as decreases or loss in sensitivity to sensory stimuli, inappropriate signaling of pain, or motor impairment.

Following nerve injury, there are signals sent back to the dorsal root ganglion (DRG) that cause a shift in gene transcription, facilitating the start of repair⁶. These include proteins like β -tubulin for example, which is important for allowing the growing tip of axons, also known as the growth cone, to advance towards targets⁷. The distal segment of the nerve undergoes Wallerian-like degeneration, which is the process of breakdown of the distal axon segments and this is mediated by a variety of proteases including calpains and E3/E4 ubiquitin ligases mediating protein degradation⁶. Structural neurofilament lattices are broken down and this helps to mediate the breakdown of these axons^{6,7}.

Clearance of the disconnected axon tracks is critical to allow for new axons to be formed. This is mediated by Schwann cells (SCs) that normally function to myelinate

and support undamaged axons. They undergo a phenotypic shift which can be identified by the expression of glial fibrillary acidic protein (GFAP) and P75 (low affinity NGF receptor). They also undergo rapid proliferation and become phagocytotic to help with the clearance of axon debris including growth inhibiting myelin and myelin associated glycoproteins (MAGs)⁷. SCs and macrophages release nitric oxide (NO) which is able to react with superoxide and can cause peroxidation and breakdown of myelin⁸. This creates a growth permissive environment for regenerating axons. Augmenting either the speed and efficacy of clearance of old damaged axons and their myelin or improving growth permissive gene expression within the perikarya of the DRG are approaches that can be used to improve the regrowth in damaged nerves.

In this study, we are using molecular approaches in order to aid regeneration, however there are other means to improve outcomes after injury such as surgical interventions or electrical stimulation of damaged nerves^{9,10}. Electrical stimulation has been previously shown to improve indices of regeneration including the number of regeneration of axons, speed of regeneration, the myelin thickness, as well as the expression of BDNF in the spinal cord^{10,11}. Surgical techniques such as suturing of the two ends of a transected nerve have been evaluated⁹. Another surgical technique often used is using nerve grafts from a different region of the patient or from cadavers⁹. There are issues with both of these approaches such as the need for immunosuppression in patients receiving allografts⁹. There has also been research dedicated to the development of conduits that allow the nerve ends to be brought together while allowing for communication with the microenvironment outside¹². These

provide similar outcomes to autograft in non-human primates. Understanding of the importance of the microenvironment and ways of improving engraftment and axon regrowth have been implemented into the creation of conduits containing growth supportive cells or substrates^{13,14}.

The central nervous system (CNS) is well known for having hindered growth capabilities. This is partially due to inability of the neurons to transition from a transmission phenotype to one of growth. The PNS is less restricted in this transition and is better at undergoing the conversion to a regenerating phenotype. Although the PNS is better able to regenerate and grow, recovery outcomes following injury or disease are often disappointing. Recently, molecular mediators restricting the growth of neurons in the healthy PNS have been identified as barriers for regrowth. For example, Retinoblastoma 1 (RB1), and phosphatase and tensin homolog deleted on chromosome 10 (PTEN) are tumour suppressor molecules that prevent the formation of cancer in healthy cells by restricting their growth potential and division capabilities^{2,3}.

Temporary reduction in expression of these mediators have shown improved regeneration of peripheral nerves following injury^{2,3}. Further identification of other molecules responsible for the slow and restricted growth of peripheral nerves could open up therapeutic avenues. These in turn might be possible to translate into the clinic.

Tumour suppressors such as PTEN and RB1 are attractive targets as decreasing their expression causes the cell to go from a quiescent state, to one of growth and proliferation. More specifically, RB1 can prevent transition of cells into the S phase of the cell cycle by inhibiting E2F. When RB1 is phosphorylated it releases E2F which can

drive transcription¹⁵. Patients with a defective RB1 gene are prone to develop retinoblastomas, a form of eye cancer.

One cause for concern when manipulating tumour suppressors is that although the neuron will not be expected to divide inappropriately or form a tumour, the surrounding glial cells may be predisposed to transformation. Therefore, in clinical situations, caution will likely be critical when manipulating these cellular pathways. With this in mind, temporally synchronizing intervention at these molecular nodes during the period of regeneration will be critical to prevent hypermyelination, neuromas or cancer^{4,16}.

The Myc family of transcription factors have been extensively studied for their role in enhancing the formation and growth of tumours. c-Myc and N-Myc are the most well-known proteins within this family and have also been implicated heavily in fetal development^{17,18}. An example of the oncogenic potential of c-Myc was shown by Ladu et al, (2008). They classified human hepatocellular carcinoma samples into those with better or poor prognostic outcomes¹⁹. Here they found that c-Myc was upregulated strongly throughout all of the samples from individuals with poor prognostic outcomes¹⁹. This supports the role that c-Myc plays in neoplastic tissue.

The ability of dysregulated c-Myc to drive transformation and growth of cells makes it of interest to study within peripheral neurons. Understanding its role in the nervous system may point toward efficacious intervention nodes within humans with 'irreversible' neurological disorders. For example, not all patients who have retinoblastoma have a non-function RB1 gene. Instead a small subset population carry

an N-Myc mutation resulting in formation of and otherwise identical tumour²⁰. This supports the idea that the Myc family is capable of driving growth and proliferation, possibly in a similar fashion to RB1.

c-Myc is regulated through a variety of mechanisms to avoid its inappropriate signaling. For this study, we chose to focus on a competitive intrinsic inhibitor of c-Myc called Max dimerization protein 1 (Mad1). In order to function as a transcription factor, c-Myc forms a heterodimer with Myc associated factor X (Max)²¹. Mad1 inhibits c-Myc induced transcription by binding to Max and thereby preventing its interaction with c-Myc and blocking its signaling. In the present work, we focused on examining the role of c-Myc and Mad1 in the adult peripheral nervous system. Here, we used small interfering RNA (siRNA) to reduce the expression of c-Myc and Mad1 *in vitro* and *in vivo*.

2. Background

2.1 Peripheral nerve regeneration

The peripheral nervous system has a greater capacity to regenerate in contrast to the central nervous system. Despite this, the regenerative outcomes for patients with damaged peripheral nerves as a result of physical trauma or neuropathy remains poor. Regrowth of functional nerves has been improved experimentally by identification of a list of mediators important in the regrowth of axons in animal models. PTEN, Rb1, and RhoA are mediators whose suppression yields enhanced regeneration^{1,3,22}. These molecular approaches show promise and through identification of other mediators, treatment options for ramping up the regenerative potential of these neurons can be developed. There is currently a lack of regenerative treatment options in patients with nerve trauma and disease.

Peripheral nerves include axons which carry motor inputs from the ventral root and sensory axons that carry information from innervated targets to the dorsal root. The sensory axon cell bodies are organized into ganglia located at the dorsal root, thus appropriately named the dorsal root ganglion (DRG). The peripheral nerve trunk is organized into compartments. Axons and Schwann cells (SCs) are surrounded and contained within the endoneurium, which also contains macrophages, mast cells, fibroblasts and blood vessels⁶. The endoneurial compartments are then organized into

fascicles and surrounded by the perineurium, which is composed of specialized fibroblasts⁶. Fascicles are surrounded by a highly vascularized epineurium which is not tethered directly to adjacent tissues allowing for the nerve to slide during movement⁶. Following an axonotmesis injury, like a crush injury, the connective tissue and the epineurium are maintained and this does not require the surgical connection of the proximal and distal end of the nerve⁶. This contrasts with neurotmesis which involves severing of the connective tissue and this causes the retraction of the proximal and distal end from each other⁶. This is more severe and has a poor prognosis. This requires connective tissue or surgical intervention to bridge the gap between the proximal and distal stump. Neurapraxia are injuries that have focal demyelination but do not have axonal damage and have good prognostic outcomes⁶. In this study, the focus was on nerve crush, keeping the connective tissue surrounding the nerve intact.

SCs are supporting glial cells that myelinate axons and allow for saltatory conduction through nodes of Ranvier. Following injury, they are able to secrete cytokines before there is infiltration of inflammatory cells and can also provide neurotrophin support and guide newly made axons through three-dimensional space by their assembly of bands of Bungner⁶. SCs play highly dynamic roles between their normal myelinating and supportive phenotype in the uninjured PNS, and their phagocytic, axonal support and guidance phenotype in response to injury. The importance of these cells in supporting the regeneration of axons have been shown in part by Guénard et, al. (1992). They found that including SCs into conduits help improve regeneration, highlighting the importance of SCs, in nerve repair¹³.

Following damage to axons, there is an immediate and likely irreversible influx of calcium that can signal proteases and ubiquitin ligases to initiate the breakdown of axons distal to the injury⁶. Additionally, there is a retrograde signal to the perikarya that cause changes in gene expression resulting in the upregulation of regeneration associated genes (RAGs) that help mediate the regrowth of damaged axons⁷. RAGs encode proteins including β -tubulin, GAP43, HSP27, ATF3, CREB3, among a larger repertoire now identified by RNA seq studies^{6,23-26}.

This gene expression is critical for the phenotypic change from normal uninjured signal transmitting neurons, to one of recovery and growth⁴. Within lymphocytes it has been demonstrated that the total level of RNA in B-cells is dependent on c-Myc expression and therefore genes involved in axon regeneration may likewise require a concurrent rise in c-Myc activity²⁷.

Although neurons do not divide, the surrounding glial cells do. This is particularly important in the regenerative response⁶. Following injuries, Schwann cells dedifferentiate and rapidly divide. This phenotypic change allows for the Schwann cells to be able to phagocytose the products of axonal degeneration, some of which are inhibitory to regrowth^{6,28}. Successful clearance facilitates subsequent SCs guidance of the newly sprouting axons from the proximal stump of the injured nerve. Changes in the c-Myc transcription pathways may impact surrounding Schwann cells with secondary benefits on axon regrowth and recovery from injury. Manipulation and enhancement of SCs growth does support regrowth of its axon partners, for example through the netrin receptor Unc5H2 inhibition or calcitonin gen-related peptide (CGRP)

signaling^{29,30}. Recent data however have identified epithelial mesenchymal transition (EMT) processes within SCs and it is conceivable that enhancement of this process through excessive growth signaling might promote SC tumorigenesis³¹. The EMT allows cells to take on a dedifferentiated mesenchymal like phenotype, allowing for motility and wound healing³¹. Neoplastic transformation in SCs might be associated with Schwannomas and other tumours.

SCs play an important role in the regenerative response and ablation of Schwann cells leads to poor regenerative outcomes²⁸. For instance, in diabetic neuropathy, there are changes in the SCs ability to migrate and provide a supporting microenvironment for axonal regrowth²⁸. Normally, SCs help in clearance of debris in the damaged nerve and allow for creation of a supportive basement membrane for new growing axons²⁸. Following injuries, SCs undergo dedifferentiation changes that include expression of p75 (low affinity NGF receptor) and GFAP⁶. An important signaling protein in supporting the proliferation ability of activated Schwann cells is pERK³². GFAP can bind to integrin alpha v beta 8 causing downstream phosphorylation of ERK and deletion of GFAP impairs SC growth similar to the impact of an ERK inhibitor³². The SCs from GFAP null mice show reduced ability to proliferate and have lower quantities of pERK, however they maintain similar levels of unphosphorylated ERK. As reviewed later, pERK likely plays a role in phosphorylation and stabilization of Myc³². These findings suggest that c-Myc is likely to have important impacts on SC behaviour after injury.

Clements et al., (2017) showed that there are phenotypic differences between SCs proximal to the injury compared to SCs that invade into the space between the proximal and distal stump of the axons. The ability of the Schwann cells between the nerve stumps to take on an invasive phenotype is through activation of pluripotency factors and is a product of, among other things, enhanced c-Myc signaling. c-Myc has been categorized as a central player in maintaining pluripotency within stem cells (PSC)³³. This has been postulated to be a product of Myc's ability to increase mediators of cell cycle progression like cyclins and CDKs, while also repressing proteins involved in tumour suppression and differentiation³³. Not only does Myc contribute to maintaining PSCs, it can be used as a tool for retroviral infection of fibroblasts to induce pluripotency as described by Nobel laureate Shinya Yamanaka^{34,35}. The ability of Myc to reprogram cells could affect the efficacy of the phenotypic change of SCs that is essential for regeneration to progress.

c-Myc has yet to be evaluated in the context of PNS injury and disease. Within the central nervous system, Belin, S. *et al.* (2015) demonstrated that there is a reduction in c-Myc transcripts in retinal ganglion cells (RGCs) following an optic nerve crush. Furthermore, if they over expressed c-Myc, optic nerve axonal regeneration was enhanced and could synergize with PTEN for superior optic nerve regrowth³⁶. To enhance c-Myc in the PNS, my strategy is to explore Mad1 knockdown to potentially remove a brake on c-Myc, dysregulate it and allow it to promote more robust growth that is required for recovery of damaged nerves.

2.2 Myc

2.2-1 Myc structure and function

The Myc family of proteins was identified by the discovery of a viral gene encoded by the avian retrovirus MC29 transforming virus that was named v-Myc after its association with the induction of myelocytomatosis in chickens^{37,38}. Following this work, a mammalian cellular homologue was identified and labeled c-Myc for Cellular Myc³⁸. Shortly thereafter, other members of the Myc family, N-Myc and L-Myc were added to the family as oncogenic proteins^{39,40}. The Myc family members regulate the same sets of genes and they are able to compensate for each other⁴¹. The primary difference between each member is their expression patterns and regulation during and after development⁴¹.

The Myc family have been of interest because dampening its oncogenic potential may be associated with new forms of cancer therapy^{17,21}. Myc is overexpressed or dysregulated in a wide variety of malignant tumours and knocking down c-Myc attenuates tumour size in xenografted nude mice⁴². Oncogenic activation of the c-Myc gene can occur through a variety of mechanisms including: increased protein and RNA stability, enhanced translation, or increased gene amplification³⁸. Additionally, expression of c-Myc can influence the size of cells, for example when manipulating the *Drosophila* orthologue, *dmyc*^{17,18,38}. This effect is not exclusive to simple organisms, but is also observed in complex mammalian systems. Overexpression of c-Myc in vertebrates results in larger sized hepatocytes and B-lymphocytes^{21,43}

The Myc family of proteins contain a basic helix loop helix domain (bHLH), a common feature of many transcription factors^{17,44,45}. This bHLH domain allows for interactions with a key binding partner Max⁴⁶. Together, these proteins are capable of binding to DNA and recruiting other proteins such as histone demethylases and histone acetyltransferases^{47,48}. These histone modifications change the structure of chromatin allowing for certain genes to become more accessible by transcription machinery. For example, if Myc is silenced within oligodendrocytes, there is an increase in the histone methylation of Myc target genes, reducing their transcription, indicating the important role that histone modification plays in Myc signaling⁴⁸. This silencing pathway is common to a number of transcriptional genes.

Myc regulates a variety of genes involved in metabolism, protein synthesis, cell cycle regulation, cell adhesion and cytoskeletal proteins²¹. Additionally ribosomal and mitochondrial biogenesis related genes are also upregulated by Myc²¹. Through single neuron analysis, it has been demonstrated that following injury of motor neurons in *C. elegans*, neurons that fail to increase the number of mitochondria in the injury site have poor regenerative outcomes⁴⁹. Along these lines in the nervous system, enhancing Myc signaling might augment biogenesis of mitochondria with secondary benefits to neurons and their axons. Optimized mitochondrial function likely helps to attenuate neuropathies in disease and may support regeneration of axons.

The Myc family has been largely implicated in early neurodevelopment. Knockout of either N-Myc or c-Myc is embryonically lethal, and conditional knockout of either or both result in microcephaly⁵⁰. A double conditional knockout of both N-Myc

and c-Myc can cause an overall reduction of 60% of total brain weight⁵⁰. This is further supported by observations made in the developing lens. Cre recombinase driven knockdown of c-Myc in the lens of developing rodents show impaired lens organogenesis and result in poor formation of the lens⁵¹. The authors note that this is a consequence of reduced proliferation and not due to reduced cell survival.

c-Myc has been estimated to directly and indirectly regulate 15% of all genes in a wide range of organisms from *Drosophila* to *homo sapiens*²¹. There is a range of functions that c-Myc target genes encode for including cell cycle, metabolism, protein biogenesis, and cell adhesion²¹. An example is the CDK/E2F/RB pathway. In nasopharyngeal carcinoma, if c-Myc is knocked down, cyclin D1, CDK2, pRB, and E2F3 are downregulated, and is associated with reductions in the proliferation of transformed carcinoma cells⁴².

One major function of Myc within cells is to allow for acceleration into the S-Phase, or DNA synthesis phase in cells that would otherwise be in a quiescent state⁴². Consistent with this finding it has been shown that cell cycle related genes such as Cdk2, Cdk4 and Cdk6, along with levels of Cdk Activating kinase (CAK) are increased with c-Myc expression and Cdk inhibitory kinase (Wee1) is reduced⁵². Cdk-cyclin complexes are needed for progression through the cell cycle, and by increasing levels of the proteins and reducing inhibitory mechanisms on Cdks, c-Myc promotes rapid entry into the S-phase. Although neurons do not divide, traversing the S phase checkpoint through enhanced signaling of E2F following Rb1 knockdown has been previously shown to enhance regeneration³. This is because E2F is normally inhibited by RB1 and

following activation of signal transduction pathways including growth factor signaling, RB1 becomes hyperphosphorylated and inhibited by CDK4, permitting E2F1 to mediate its transcriptional factor activity, allowing for growth signaling¹⁵. Therefore, by knocking down RB1, E2F1 signaling can be enhanced without CDK4 signaling. Myc's ability to influence the cell cycle may show a similar effect to RB1 knockdown.

2.2-2 -Myc and apoptosis

Along with its transcriptional functions, excessive c-Myc signaling can initiate apoptosis^{17,53,54}. Excessive Myc signaling in the absence of growth factors or nutrients is capable of driving apoptosis²¹. Considering its intense association with many types of cancer, this mechanism is protective in preventing tumours from forming under normal conditions. The full pathway has not been completely elucidated, however there are some mediators that have been identified to play a role in Myc mediated apoptosis. Bcl-2 associated X (Bax) is a proapoptotic protein that has been shown to increase upon c-Myc activation⁵³. Bax dependent apoptosis in c-Myc overexpressing mutants can be ameliorated by knockdown of Bax³⁸. This mechanism to prevent c-Myc neoplastic growth in cells is capable of shifting the balance of pro- and anti-apoptotic signals towards programmed cell death.

In the context of the nervous system, c-Myc's pro-apoptotic role could result in a reduction in the survival of neurons, and thus an abrogated growth response. A study performed by Murphy et al., (2008) provides evidence that there is a threshold for the

level of c-Myc activation necessary to drive apoptosis. This study used an inducible c-Myc system where they coupled c-Myc to an estrogen receptor (MycER) such that addition of tamoxifen would cause translocation of the chimera protein to the nucleus⁵⁵. The level of c-Myc activation in this study was insufficient to trigger apoptosis, however it did prime the apoptotic machinery such that an additional noxious stimuli would cause apoptosis⁵⁵. Based on this data, whether or not a cell commits to apoptosis is likely dependent on the cellular environment and the extent of Myc signaling. A caveat for the work presented in this thesis therefore is that the combination of injury and c-Myc signaling might promote undesirable neuron or Schwann cell apoptosis. We addressed this concern, by using Terminal deoxynucleotidyl transferase(TdT) dUTP nick-end labeling (TUNEL) assay to look for evidence of apoptosis. Following apoptosis, DNA undergoes extensive fragmentation. Using the TdT enzyme, fluorophore or other conjugated dNTPs can be added to the ends of each fragment and can be detected. We have found that the siRNA induced knockdown of Mad1 was insufficient to cause neuronal cell death, possibly indicating that increased cellular levels of Myc are unable to cause apoptosis in neurons.

2.2-3 Other c-Myc interacting proteins

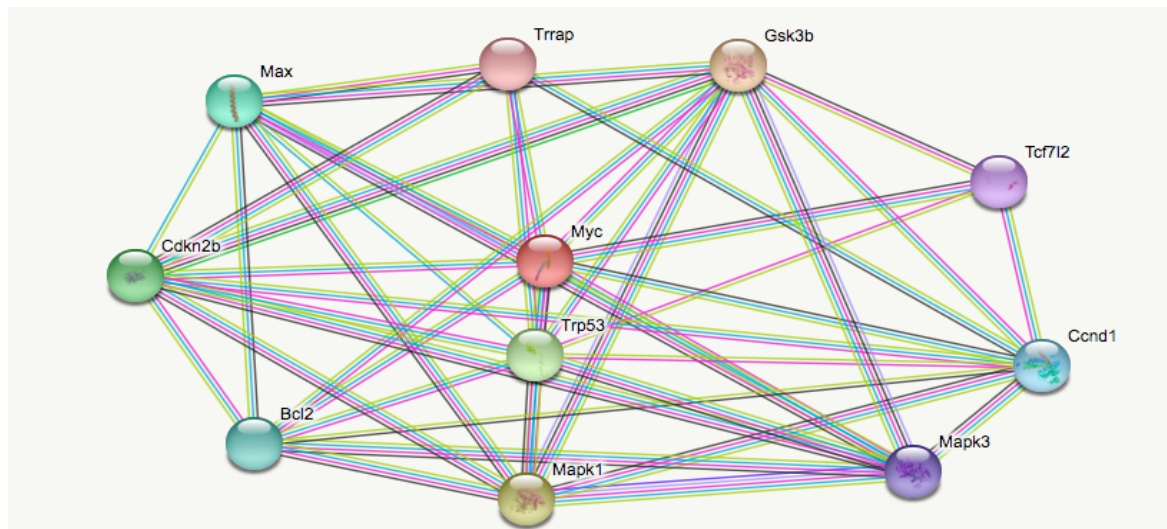


Figure 1: A string analysis of c-Myc interacting proteins in *Mus musculus*. The coloured circles identify proteins with their identification above. The lines or “strings” connecting each circle shows an interaction between the proteins. [Retrieved from string-db.org through String V10.5 software] ⁵⁶

Myc is capable of interacting with other proteins in addition to Max. Figure 1 is a STRING analysis showing the 10 known nodes that c-Myc interacts with⁵⁶. Firstly, glycogen synthase kinase 3 β (GSK3 β) is a negative regulator of c-Myc and in the PNS prevents growth cone extension⁶. It causes phosphorylation of c-Myc on Thr 58 and is associated with decreased c-Myc stability and degradation^{57,58}. GSK3 β knockdown promotes axon regeneration within the CNS, and we can speculate that this may be in part through enhanced c-Myc stability⁵⁹. Furthermore, GSK3 β can also target and activate adenomatous polyposis coli (APC) signaling which has been shown to be a negative regulator of c-Myc transcription⁶⁰. Along these lines, our laboratory has identified enhanced nerve regeneration in the setting of APC knockdown⁶¹. One can speculate that with reduced stability and transcription of c-Myc through GSK3 β

activity, there will be an increased propensity of Mad1 to dimerize with Max, allowing for transcription repression and chromatin remodeling.

Another interacting partner of Myc is the anti-apoptotic protein Bcl-2. The BH4 domain of Bcl-2 has been shown to interact with the MBII domain of c-Myc⁶². Similar to c-Myc, Bcl-2 is an oncogenic protein that may become upregulated in cancers and increase resistance of cancer cells to apoptotic processes following DNA damage⁶³. It prevents cell death through blocking release of cytochrome c and apoptosis inducing factor (AIF) from the mitochondria, and prevents depolarization of the mitochondrial membrane⁶⁴. Bcl-2 has also been shown to interact with c-Myc to increase its transcriptional activity and to prevent DNA damage repair⁶². Within the nervous system, Bcl-2 declines in peripheral facial motor nerves following transection⁶⁵. Thus a potential c-Myc and Bcl-2 interaction in the peripheral nervous system may have some bearing on regenerative behaviour of peripheral neurons .

Mitogen activated protein kinases (MAPK/ERK1,2) are responsible for classical mitogen induced cell growth and involve upstream activation of Ras. It has been shown that phosphorylation of Myc on the N-terminal Ser 62, likely by ERK, stabilizes Myc and causes its accumulation⁵⁷. This contrasts with its phosphorylation by GSK3 β on Thr 58 which signals it for degradation⁵⁷. In cells treated with an ERK inhibitor, there is a reduction in the levels of c-Myc proteins, along with reduction in phospho-c-Myc⁶⁶. The ERK1/2 pathway has been shown to be an important mediator associated with neurotrophin signaling and this may be partially attributed to ERK-induced Myc stabilization⁶⁷. Moreover, NGF has been shown to increase phosphorylation of GSK3 β

on serine 9 through the PI3K-Akt pathway, rendering it inactive, and this in collaboration with Myc phosphorylation by ERK1/2, could favor its accumulation^{6 68}. Taken together there may be a central role for intrinsic Myc activity in neuronal plasticity required for peripheral nerve regeneration. Figure 2 shows an overview of the the described interactions.

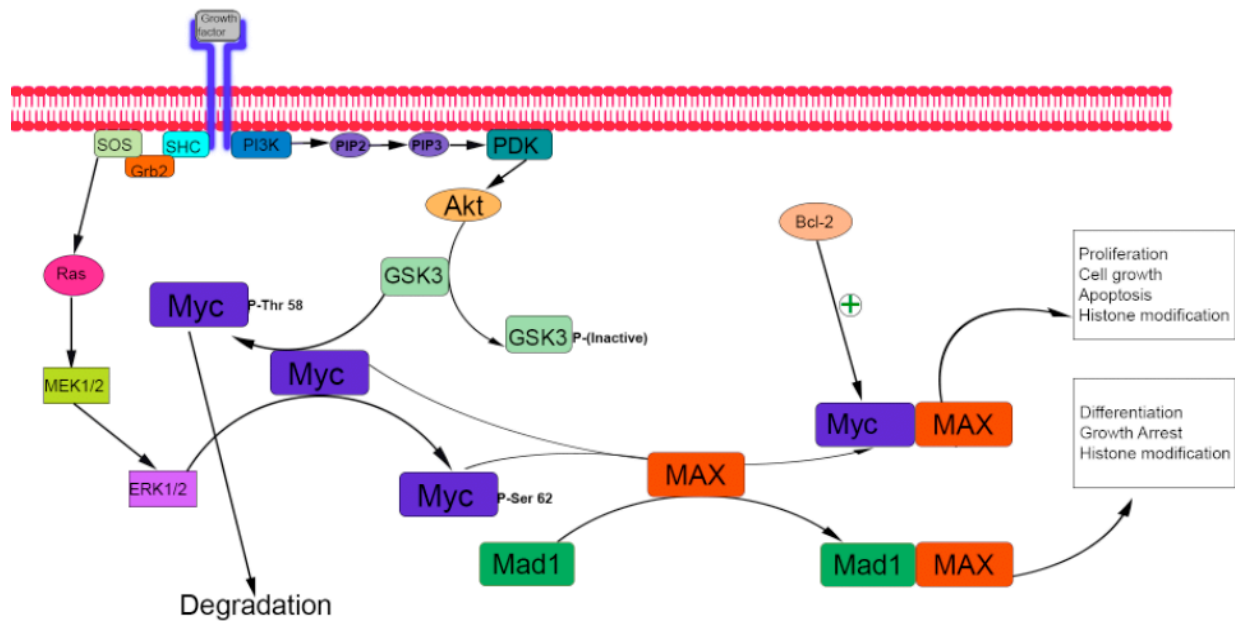


Figure 2: Growth factors including NGF will interact with the extracellular domain of their respective receptors. This will be transduced through the membrane and cause intrinsic tyrosine kinase activity. This will result in recruitment of Src homology 2 (SH2) domain containing proteins to the receptor such as SHC. This will bind an adaptor protein like growth factor receptor bound protein 2 (Grb2). This will cause recruitment of son of sevenless (SOS), a guanine exchange factor which will activate Ras. Ras activation will cause stimulation of mitogen activated kinase kinase (MEK1/2) and results in mitogen activated kinase (ERK1/2) becoming active. Myc can then be phosphorylated on serine 62 by ERK1/2 and this causes accumulation and stabilization of the protein. Bcl-2 can further increase the accumulation of Myc. Myc can then interact with Max through its bHLH domain and these dimers can move to the nucleus and bind to enhancer box sequences on target genes. Activation of Myc target genes will lead to growth, proliferation, apoptosis, and histone modifications such as demethylation and histone acetylation. Mad1 can antagonize this interaction by binding to Max thus preventing c-Myc target genes from being transcribed and causes different gene silencing histone modifications such as deacetylation and methylation. Additionally, phosphoinositide 3-kinase (PI3K) can become activated and this will

convert phosphatidylinositol 4,5 bisphosphate (PIP₂) to phosphatidylinositol 3,4,5 trisphosphate (PIP₃) which is a prerequisite for phosphoinositide-dependent kinase (PDK) activation. PDK can phosphorylate protein kinase B (Akt) and subsequently cause its activation. Akt can inactivate glycogen synthase kinase 3 β (GSK3 β) which normally will phosphorylate Myc on threonine 58, targeting for its degradation.

2.2 Mad1

Mad1 is a competitive inhibitor that binds to Max, thus preventing c-Myc from inducing transcription. Like Max and c-Myc, Mad1 also has a bHLH domain allowing Mad1 to dimerize with Max in a similar fashion as c-Myc²¹. When these heterodimers form, they not only prevent c-Myc derived transcription through competitive inhibition, but can also bind to the same E-box sequences as the c-Myc/Max dimers. Once bound, the heterodimer can recruit Sin3a/3b to the mSin domain on Mad1⁶⁹. This acts as a scaffold protein permitting histone deacetylases to join the complex and causes chromatin remodeling. This prevents the access of these genes by the transcription machinery and thus causes transcriptional repression. Additionally, Mad1 acts by competitively binding for Max at the bHLH domain, thus preventing c-Myc dimerization²¹. Therefore, it counteracts expression of c-Myc target genes.

The Mad family of proteins (Mad1, MXI1, Mad3, Mad4) are associated with differentiation during fetal development⁷⁰. Of these proteins, Mad1 is the most highly expressed protein in terminally differentiated tissue⁷⁰. For the purposes of this thesis therefore, it is the most relevant for considering in the peripheral nervous system⁷⁰. In order for normal development to occur, there needs to be a balance of c-Myc expression in tissues to allow for growth, and Mad1 to allow for differentiation. Mad1 therefore

functions to dampen growth by blocking c-Myc and this will also cause the differentiation of tissue. For instance, in oligodendrocyte progenitor cells (OPC), there is an inverse relationship between the expression of myelin basic protein and c-Myc levels⁴⁸. This coincides with an overall reduction in c-Myc protein expression in the corpus callosum and in developing white matter, and is likely concurrent with heightened expression of Mad1 based on observations during development⁴⁸. Furthermore, it is possible to block differentiation of cells by increasing the level of c-Myc signalling, further supporting the importance of balanced Mad1 and c-Myc signalling specifically during neurodevelopment⁷¹.

Dysregulating c-Myc through manipulating Mad1 in the peripheral nervous system may increase the growth potential in neurons through enhanced activation of growth stimulating pathways. Foley et al. (1999) knocked out Mad1 in granulocytes and stimulated with granulocyte colony stimulating factor (G-CSF) and noted that the cells had a greater proliferative capacity⁷². Neurons are post mitotic, but intrinsic activation of their plasticity through c-Myc enhancement may instead support their regenerative efforts. For this reasons, this thesis will focus on manipulating this specific target in exploring approaches to improve regeneration of adult neurons.

2.3 Max

Max is a ubiquitously expressed protein that is an important player within the Myc/Mad1/Max growth signaling axis. It may also be highly relevant in supporting growth responses in the damaged peripheral nervous system. Out of the three proteins

in this network, Max is the only member that forms homodimers, although the biological implications of this are unknown⁷³.

Like other members of this network, Max has also been implicated in neoplastic transformation. For example, loss of function mutations within the bHLH domain of the Max protein have been identified in a subset of pheochromocytoma patients⁷⁴.

Therefore it is possible that Myc dysregulation and loss of Max may contribute to tumour cell growth synergistically. An inability of Max to dimerize with Mad1 and other repressors of the signalling axis may permit unfettered c-Myc signaling.

The loss of function Max mutation also prevents dimerization with c-Myc, an outcome that might prevent transcription of c-Myc genes. There is also evidence that Myc may function independently of Max and offer transcriptional activity. Ribon et al (1994) discovered that Max was not detectable in PC-12 cells, and when these cells were stimulated with NGF there was increased levels of c-Myc and consequently, increased transcriptional activation of its targeted promoters, suggesting that Myc may be able to function independently of Max to drive growth and proliferation⁷⁵. Additionally, forced over expression of c-Myc in the absence of Max is capable of driving apoptosis independently⁷⁶. Therefore Max may have an important role in the repression of growth, a feature of potential importance in regenerating neurons.

3. Methods

3.1 Animal models

All procedures and protocols described in this thesis were independently reviewed and approved by the Health Sciences Laboratory Animal Services (HSLAS) at the University of Alberta, and adhered to the guidelines of the Canadian Council on Animal Care (CCAC). All cultures and neurite outgrowth experiments were conducted using Sprague Dawley rats (Charles River Canada). Expression data and *in vivo* studies were performed using CD1 mice (Charles River Canada). Male rodents were used for all experiments.

3.2 RNA isolation and qRT-PCR

TRIzol® reagent was used to extract the total RNA as per the manufacturer's instructions (Invitrogen Carlsbad California). One microgram of RNA was treated with DNase (Promega Madison, Wisconsin) and a High capacity cDNA reverse transcription kit (Applied Biosystems Foster City, California) to convert the RNA to its complementary-DNA (cDNA). SYBR Green fluorophore (Applied Biosystems) was used for the quantitative real-time PCR. The cycle number where the fluorescence signal crosses a fixed cycle threshold (CT) with an exponential growth of PCR product during the linear phase was recorded and using the comparative CT method ($2^{-\Delta\Delta CT}$), and relative expression values were generated. All genes of interest were normalized to expression of housekeeping genes. Primer sequences are shown below.

Mouse cMyc F: 5'-GCTGTAGTAATTCCAGCGAGAGACA-3'

Mouse cMyc R: 5'-CTCTGCACACACGGCTCTTC-3'

Mouse Mad1F: GCAAGGACAGAGATGCCTTCA

Mouse Mad1R: GTGAGCACGCCTGTTCTTTCC

Mouse Max F: AAGCGGCAGAATGCTCTT

Mouse Max R: GTTGGTGTAGAGGCTGTTGT

Rat cMyc F: GTCCTCAAGAGGTGCCATGT

Rat cMyc R: CTCGCCGTTTCCTCAGTAAG

Rat Mad1 F: GCAAGGACAGAGATGCCTTCA

Rat Mad1 R: GTGAGCACGCCTGTTCTTCTC

RPLPO F: AAGAACACCATGATGCGCAAG

RPLPO R: TTGGTGAACACGAAGCCCA

3.3 Adult sensory neuron cultures

Rats under isoflurane were euthanized 3 days following a crush to the sciatic nerve described below. Ipsilateral L4, L5, and L6 DRGs were harvested and placed in L-15 media (Gibco Waltham, Massachusetts). The DRGs were rinsed using L-15 then placed in 1mg/ml collagenase (Gibco) in L-15 and incubated at 37°C for 90 minutes. The DRGs were then dissociated into a single cell suspension by trituration. This suspension was centrifuged and the pellet was re-suspended in L-15 and poured through a 70- μ m mesh. This solution was centrifuged using a 15% bovine serum albumin (Sigma Aldrich, St. Louis Missouri) solution to separate tissue debris and Schwann cells from neurons. The pellet was then re-suspended in 200 μ l of enriched Dulbecco's Modified

Eagle Medium (DMEM) (Gibco) containing N-2 supplement (Gibco), NGF (Invitrogen), cytosine- β -D-arabinofuranoside (Sigma), penicillin, and streptomycin. Then 25 μ l of the cell suspension was added to two 4-chamber slides with 1ml of enriched DMEM in each chamber. Chambers were pre-treated with 0.1% poly-l-lysine and 10 μ g/ml laminin.

3.4 Lesioning experiment

Rodents were anesthetized using isoflurane anesthetic administered through a ventilator. The animals were then shaved and a 3 cm incision was made mid-thigh and along the sciatic notch. The sciatic nerve was exposed, then crushed for 15 seconds using a pair of forceps. The forceps were rotated 90 degrees and the sciatic nerve was crushed at this position for 15 seconds. Following crush, the incision was sutured and the animal received buprenorphine 2 times a day for 3 days in the case of the culture experiments using rats, or 5 days in the mice used for the *in vivo* studies.

3.5 Neurite outgrowth assay

Three rats received sciatic nerve crushes as specified above and allowed to recover for 3 days post crush. On the third day, rats were euthanized and ipsilateral L4, L5, and L6 DRGs were collected. Using the procedure above, a single cell solution of the DRG neurons were plated on a 4 well chamber culture plate. The media in which the cells were grown contained 20nM of Mad1, c-Myc or scrambled siRNA with HiPerfect Transfection reagent (Qiagen Hildren Germany) or in media containing DMSO or

10058-F4 (Sigma). Twenty-four hours following plating, these cells were fixed using 4% paraformaldehyde and were blocked using 5% BSA, and 0.3% TX-100 in PBS. Next the primary antibody solution containing 1:200 Mouse anti-NF200 (Sigma) antibody and 3% BSA was added to each well. The slides were then rinsed using PBS and the secondary antibody containing 1:100 anti-Mouse antibody conjugated to Cy3 (Sigma) was added. Cells were then mounted using Vectashield mounting media containing Dapi (Vector Laboratories, Burlingame, California). Cells were imaged and images were taken of every neuron within each of the wells. Neurons were then analyzed using NeuroMath⁷⁷ software to calculate neurite lengths of each neuron. Number of sprouted neurons were manually counted from the images that were used in the Neuromath software.

3.7 Electrophysiology

Electrophysiology was performed as described in our previous studies³. Motor and sensory conduction measurements were obtained under isoflurane anesthesia. Motor nerve conduction were performed by recording at the interosseous foot muscles and stimulating at the sciatic notch and the knee. Sensory conduction was measured by stimulating at the toes and recording at the knee. A single supramaximal stimulation with a pulse width of 100 microseconds was provided for all measurements. Near nerve temperature was controlled throughout measurements and warmed by heat lamp (37.0 ±1.0 degrees Celsius). Baseline testing was performed before sciatic injury, and then measurements were taken again at 14 and 28 days post-crush.

3.8 Hargreaves Behavioral Measurements

Withdrawal latency when exposed to a thermal stimulus was measured using a Hargreaves apparatus⁷⁸ as described here in previous work³. Animals were contained within individual compartments and then placed on a plexiglass platform. A heating light was then placed under the hind paw of the mouse and the withdrawal latency was measured. Bilateral testing was performed in triplicates. Each trial did not exceed 30 seconds. Testing was performed at baseline, 14 days post crush, and 28 days post crush.

3.9 Von Frey Measurements

Mechanical force threshold measurements were taken using Von Frey filaments, similar to previous work³. Mice were placed within chambers on top of a metal mesh with holes that permitted passage of the filament to contact the animal's plantar hind paw. The filaments were pressed against the animal's paw and if no withdrawal and shaking of the paw was elicited, the next larger caliber filament that provided more force would then be applied until animals showed a response three times out of five total tests. Testing was performed at baseline, 14 days post crush, and 28 days post crush

3.10 Western Blot

Protein was extracted from DRG sensory neurons and concentration was quantified using the Bradford assay. Twenty-five μg of denatured protein lysate was

applied to an SDS page. The gel was run using 75 volts until the protein bands reached the resolving gel then the voltage was adjusted to 100 volts until the bands reached the bottom of the gel. Proteins were transferred from the gel to a PVDF membrane over 2 hours using 100 volts. Membranes were then incubated with blocking solution containing 5% powdered milk. Primary antibodies (Rabbit c-myc 1:500 (Novus biologicals Littleton Colorado), Rabbit Max 1:500 (Thermo Fisher Waltham Massachusetts), Rabbit Mad1 1:500 (Sigma) were incubated overnight at 4°C in 5% Bovine serum albumin (Sigma) in TBST. Beta tubulin (1:1500) was used as a loading control. Blots were then visualized using 1:3000 goat anti rabbit HRP (Life Technologies Carlsbad, California) or goat anti mouse HRP (Life Technologies).

3.11 Immunohistochemistry

DRGs were harvested from the L4-L6 levels and placed in Zamboni's, solution overnight at 4 degrees Celsius. Samples were then rinsed with PBS three times and stored in 20% sucrose overnight at 4 degrees Celsius. DRGs were embedded into OCT compound and sectioned at 10µm onto glass slides. Slides were then blocked using 1% bovine serum albumin, 10% goat serum, 0.3% Triton-X100, 0.05% tween 20 and 0.05% sodium azide. Slides were incubated at 4 degrees Celsius overnight using the following primary antibodies: rabbit anti Mad1 (1:100, Sigma), Rabbit Anti c-Myc (1:100, Novus biologicals), Rabbit anti-Max (1:100, Sigma), and mouse anti-Fibrillarin (1:50, Santa Cruz Dallas, Texas). Following primary antibody incubation, slides were rinsed and

incubated with secondary antibodies for 1 hour at room temperature. Secondary antibodies were anti rabbit Alexa 488 (1:200, Life technologies Carlsbad, California) and anti-mouse Cy3 (1:200 Sigma). Following incubation with secondary antibodies, slides were rinsed with PBS, and coverslips were mounted using Vectashield® (Vector Laboratories) with Dapi. Slides were visualized using a Leica SP5 confocal microscope.

3.12 In vivo delivery of siRNA and electroporation

Following sciatic nerve crushes, animals received an siRNA solution containing 5ul of 20uM siRNA (Mad1, c-Myc, or scrambled), 15ul HiPerfect (Qiagen) transfection reagent, and 30ul saline for 3 days a week for 4 weeks. The solution was injected to the sciatic notch near the crush site and the leg was then electroporated using the BTX Harvard ECM 830 electroporation apparatus (BTX, Holliston Massachusetts). Five 50ms pulses of 25 volts separated by 1 second were applied. Electrodes were placed at the site of the injury, such that the positive electrode was on top of the leg and the negative was placed below. The injury site was marked with sutures and injections were administered by inserting the needle half a centimeter below the skin.

4. Results

4.1 Expression data

4.1-1 *c-Myc* expression in injured and uninjured DRGs

Firstly, we wanted to confirm expression of *c-Myc*, *Mad1* and *Max* within the peripheral nervous system and evaluate the level of expression when comparing the dorsal root ganglion in an intact state (uninjured) and a regenerating state (injured). We found that key components of this critical signaling pathway were present within the DRG. Following 12, 36 and 72 hours after the sciatic nerve was crushed, we performed qRT-PCR to analyze the level of *c-Myc* transcription. There was no change at 12 hours following crush. Interestingly, there was an early stage reduction in the level of *c-Myc* mRNA 36 hours post crush (Figure 3A). This normalized to levels similar to the contralateral side at 72 hours post crush in these animals. Next we wanted to investigate if these changes were reflected in the protein concentration within DRGs (Figure 3B-C). There were no significant differences within the DRG protein lysates when comparing 36 hours and 72-hour time points. We confirmed the presence of *c-Myc* within the DRG and within cultured adult DRG neurons by immunohistochemistry (Figure 3D,E). In the DRG there was cytosolic staining of *c-Myc* within neurons regardless of if they were larger caliber with prominent NF200 expression, indicating expression in both large and small neuron categories. A proportion of neurons displayed nuclear staining (Figure 3D), an important feature to verify given the role that *c-Myc* plays as a transcription factor. Within cultured neurons, *c-Myc* was primarily located within the cell

body/perikarya and not identified at the growth cones or within the neurites (Figure3E).

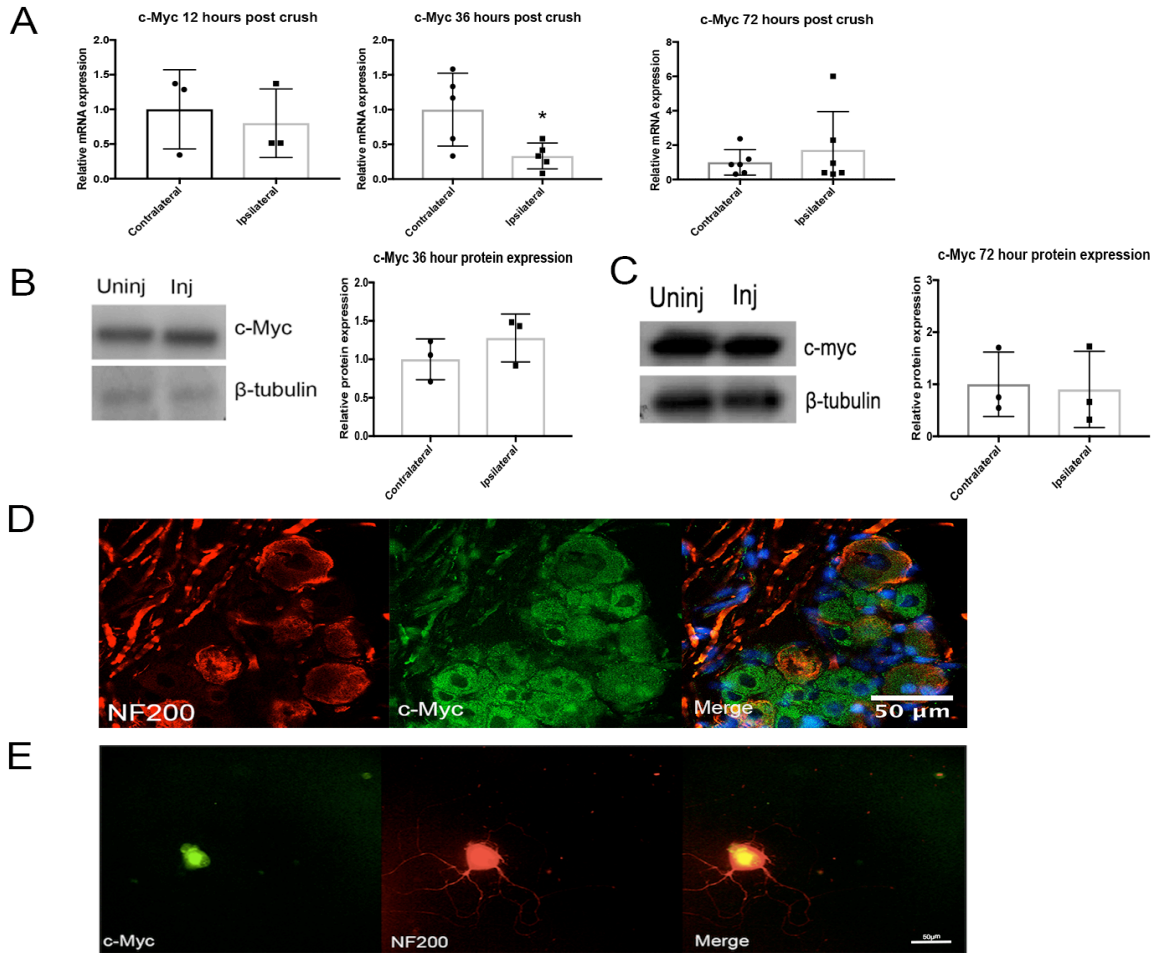


Figure 3: c-Myc is expressed in the dorsal root ganglion. (A) qRT-PCR data of c-Myc mRNA normalized to housekeeping genes in both injured and uninjured mouse DRGs at 12, 36, and 72-hour time points (12 hours n=3, 36 hours n=5, 72 hours n=6) (*P<0.05, unpaired Students t test n=6). (B) Western blot analysis comparing the protein expression of c-Myc within DRG neurons at 36-hour post injury (single example shown) with densitometric quantification normalized to the contralateral side (n=3). (C) Western blot of injured and uninjured DRG neurons comparing protein levels at 72-hour post injury (single example shown) and quantified by densitometry normalized to the contralateral side (n=3). (D) Immunohistochemical staining for NF200 (red) and c-Myc (green) of control uninjured dorsal root ganglion sections. Scale bar is equivalent to 50 μ m. (E) DRG neuron in culture stained with c-Myc (green) and NF200 (red). Bar=50 μ m

4.1-2 Max expression within injured and uninjured DRGs

Max is another key mediator of this network. We characterized the expression of Max at 12, 36, and 72 hours after nerve injury and compared the mRNA expression at these time points with uninjured control tissue (Figure 4A). There were non-significant fluctuations of the mRNA occurring at all time points. Histologically, there was staining of Max within all neurons within uninjured DRGs (Figure 4B). Given the importance of this protein in growth and development, the ubiquitous expression of this protein in all neurons is expected. Similar to other members of this signaling axis, there was also expression of Max located within the nucleus of a proportion neurons (Figure 4B lower).

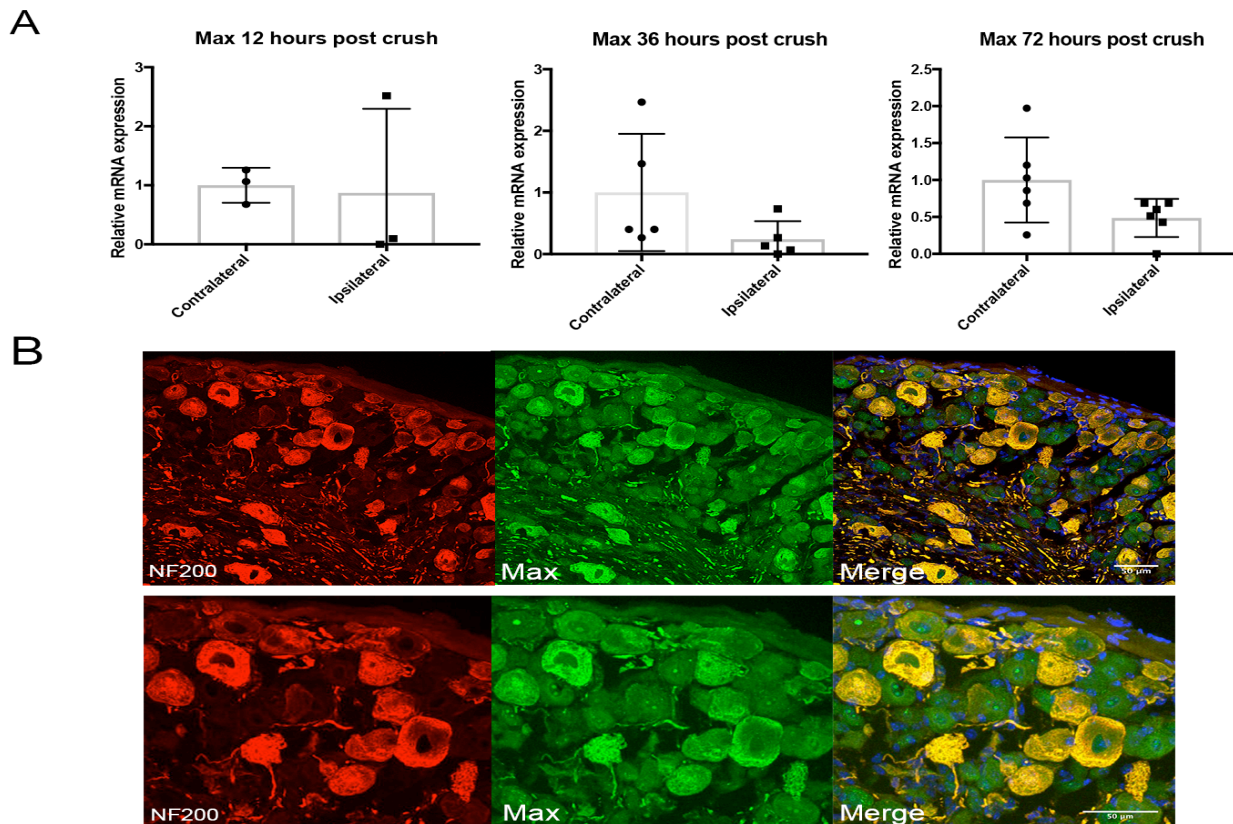


Figure 4: Max is expressed within the DRG. (A) qRT-PCR analysis of Max comparing injured with contralateral DRGs of animals receiving a high sciatic crush 12, 36 and 72 hour post injury (12 hours n=3, 36 hours n=5, 72 hours n=6). Values were normalized to the contralateral side (B) Immunohistochemistry of uninjured DRG sections staining for Max (green) and NF200 (red). Scale bar indicates 50 μ m. The lower panel is a zoomed in portion of upper panel. Bar= 50 μ m

4.1-3 *Mad1* expression within injured and uninjured DRGs

Next we characterized the expression of Mad1 within neurons. We examined qRT-PCR of injured vs uninjured DRGs at 12, 36 and 72 hours and found that there was no significant difference between these groups at any time points (Figure 5A). The expression of Mad1 protein at 72 hours also showed no difference (Figure 5B). We confirmed expression of Mad1 within DRG neurons through immunohistochemistry of DRG tissue (Figure 5C) and cultured DRG neurons (Figure 5D). Within the DRG, similar to the c-Myc expression, there was both cytoplasmic and nuclear staining. Additionally, the DRG neurons harvested and studied *in vitro* showed Mad1 expression only within the cell body and not within the projections (Figure 5D).

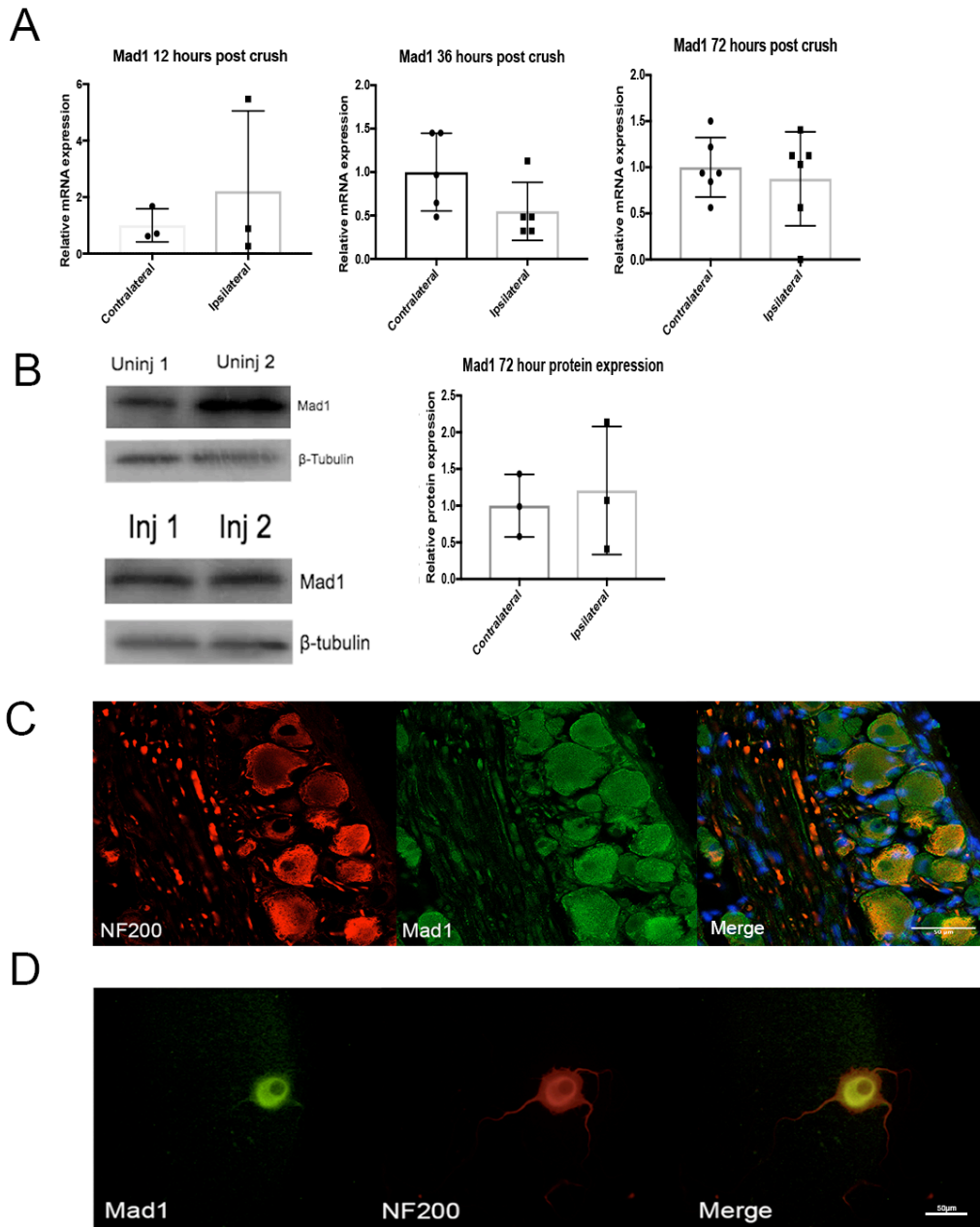
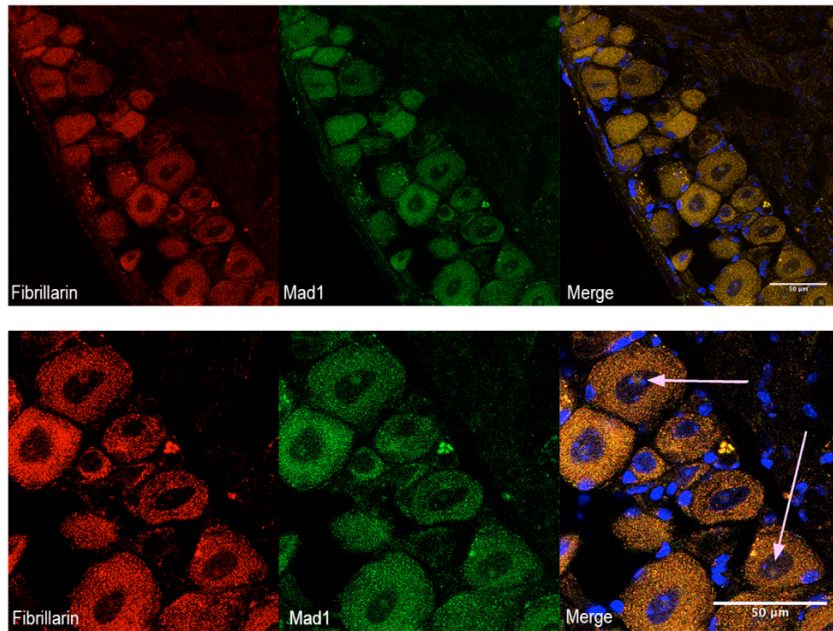


Figure 5: Mad1 is present in the DRG and its expression does not fluctuate following injury. (A) Mad1 qRT-PCR of DRGs taken at 12, 36, and 72 hours post crush. Values were normalized to the contralateral side. (12 hours n=3, 36 hours n=5, 72 hours n=6)(B) Western blot analysis probing for Mad1 protein at 72 hours post crush with values normalized to the contralateral side (n=3). (C) Immunohistochemistry of DRG sections staining for Mad1(green), NF200 (red), and DAPI (blue). Scale bar indicates 50µm (D) Immunohistochemistry of adult DRG neurons stained with Mad1(green) and NF200 (red). Scale bar is equivalent to 50µm.

4.4 Mad1 expression within the nucleolus of neurons

We next evaluated the localization of Mad1 within the nucleolus. Previous studies have shown that Mad1 is capable of relocating to the nucleolus to regulate the transcription of rRNA for ribosomal biosynthesis⁷⁹. This relocation was reported to reduce the quantity of rRNA⁷⁹. Through immunohistochemical means, we first confirmed that Mad1 was in fact able to localize to the nucleolus through co-staining with fibrillarin, an o-methyltransferase protein specific to the nucleolus (Figure 6A). Next to determine if Mad1 sub cellular localization to the nucleolus was changed in response to axonal injury, we counted the Mad1 positive nuclei in injured and uninjured DRG neurons (Figure 6B). We found that there was no significant change in the number of Mad1 positive nuclear staining between the injured and uninjured DRGs. A caveat to this experiment was that nucleolar specific signal within the nucleus was not routinely possible to ascertain for accurate counting, limiting our analysis to overall nuclear expression.

A



B

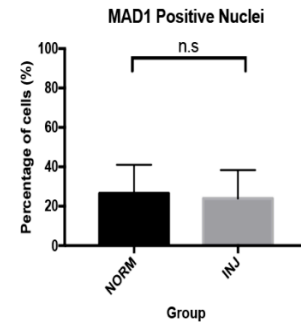


Figure 6: Mad1 is localized to the nucleolus. (A) Immunohistochemical staining of Mad1 (green), fibrillarin (red) and DAPI (blue). The lower panel is a zoomed in portion of the top panel and has arrows indicating the co-localization of fibrillarin and Mad1. Bar = 50 μ m. (B) Quantification of Mad1 positive nuclei of normal and injured DRG sections determined by immunohistochemistry (n=3). Note that DAPI also stains non-neuronal cells.

4.2 Knockdown of Mad1 and c-Myc *in vitro*

In preparation for *in vitro* knockdown studies, we first determined the adequate dose of siRNA required to successfully knockdown c-Myc and Mad1 in adult sensory neuron cultures (Figure 7). DRGs from two rats were pooled together for each experiment to ensure adequate cell numbers were available and would provide enough RNA for accurate qRT-PCR. These cultures were maintained for 24 hours in media containing two doses of siRNA (20nM and 40nM). We found that in both cases, c-Myc and Mad1 could be significantly knocked down within sensory neurons using 20nM

siRNA(Figure 7A,C). Our cultures using 40nM concentration revealed a greater variation between measurements and yielded non-significant knockdown in these cultures (Figure 7B,D). The 20nM concentration of siRNA was used going forward into neurite outgrowth assays.

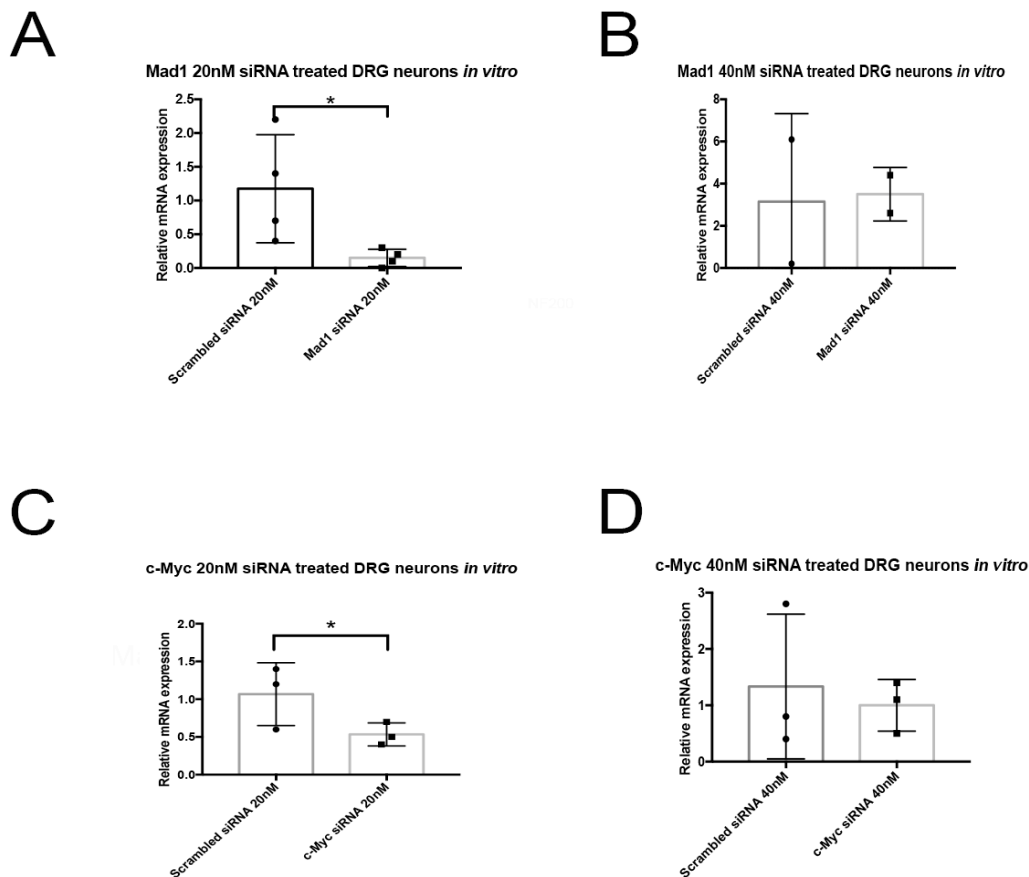


Figure 7: (A) qRT-PCR analysis of Mad1 in adult DRG cultures treated with 20nM of Mad1 or scrambled sequence siRNA(* $P < 0.05$, unpaired students T test $n = 4$). (B) qRT-PCR analysis of Mad1 in cultures treated with 40nM of Mad1 or scrambled sequence siRNA ($n = 2$). (C) qRT-PCR analysis of c-Myc in cultures treated with 20nM of c-Myc or scrambled sequence siRNA(* $P < 0.05$, unpaired students T test $n = 3$). (D) qRT-PCR analysis of c-Myc in cultures treated with 40nM of c-Myc or scrambled sequence siRNA ($n = 3$).

4.3 c-Myc and Mad1 knockdown and neurite outgrowth

4.3-1 *Mad1 Knockdown improves neurite outgrowth*

Next, we investigated the effect of our Mad1 siRNA treatment on pre-injured adult sensory neuron cultures and their ability to grow neurite projections. We first injured the sciatic nerves of 3 rats by nerve crush and on day 3, DRGs from level L4, L5, and L6 were harvested and cultured. Twenty-four hours later, the cells were fixed, and stained for neurofilament 200 (NF200) and analyzed using Neuromath software [<http://www.wisdom.weizmann.ac.il/~vision/NeuroMath/>] (Figure 8A)⁷⁷. Neurons treated with Mad1 siRNA showed an increase in the length of neurites per neuron compared to scrambled treated control cultures (Figure B, E). Furthermore, we also found a substantial increase in the proportion of neurons with neurite sprouts following treatment of Mad1 siRNA (Figure 8C). The longest single neuron neurite length measured by the neuromath software was similar between cultures (Figure 8D). The number of branches per neuron in cultures treated with Mad1 siRNA had a trend towards increased branching ($P=0.066$) (Figure 8E). Figure 8F shows a comparison of the immunohistochemical staining with NF200 to outline neurite growth in both treatment groups illustrating the heightened growth on neurons exposed to Mad1 siRNA.

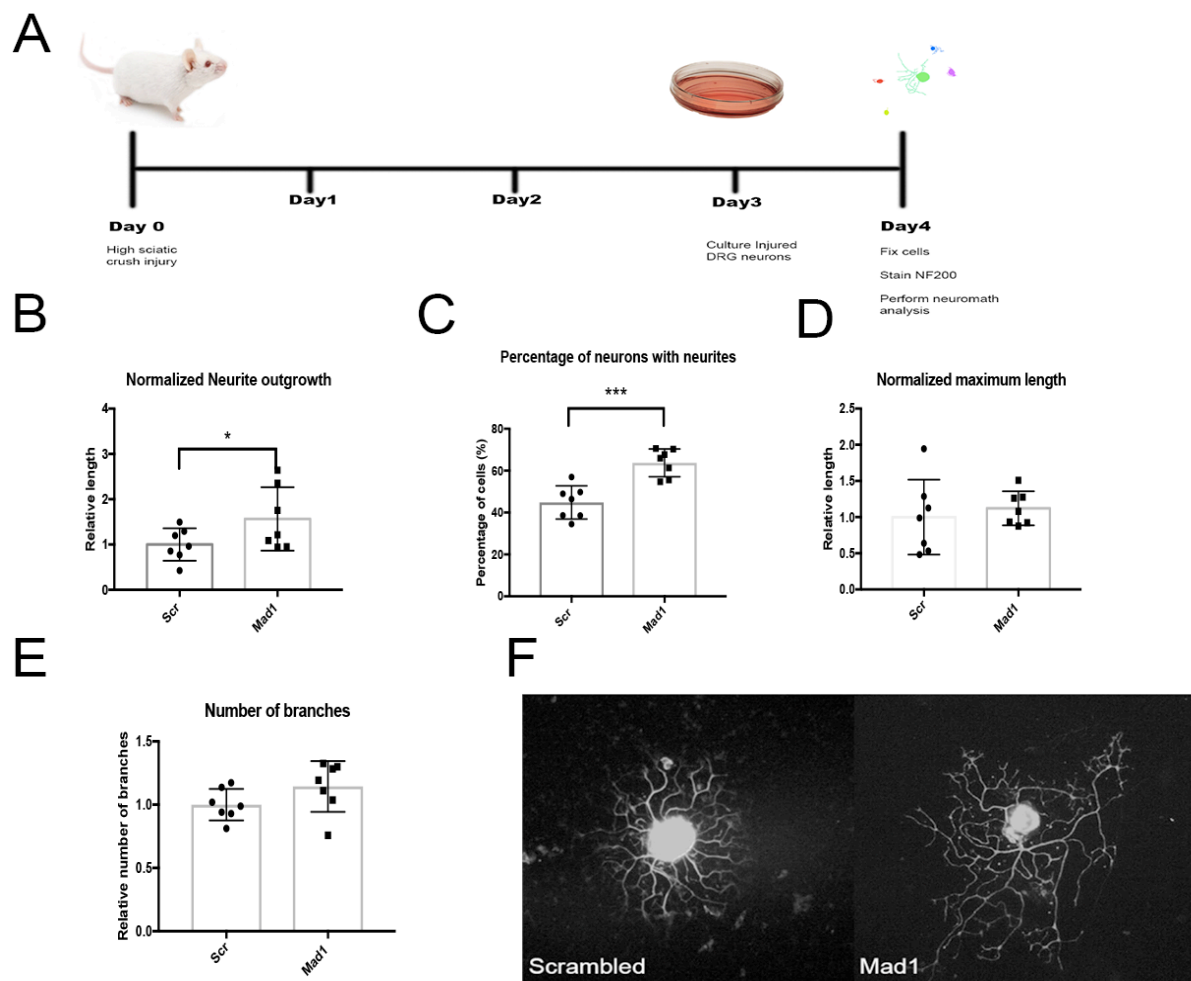


Figure 8: Mad1 knockdown improves neuron growth *in vitro*. (A) Time line for *in vitro* regeneration experiments. On Day 0 animals surgically had their sciatic nerve crushed. At Day 3, L4, L5, L6 DRGs were harvested and purified into a single cell suspension. The cultures were allowed to grow for 24 hours and on day 4 the cells were fixed with 4% paraformaldehyde, stained with NF200 and visualized using a microscope where images were collected of all neurons and were analyzed using NeuroMath software⁷⁷. (B) Neurite extension of cultures treated with 20nM Mad1 or scrambled siRNA. Values were normalized to the outgrowth of the scrambled treated cultures (* $P < 0.05$ unpaired students t-Test $N = 7$). (C) The population of neurons that sprouted compared to total number of neurons in cultures treated with 20nM Mad1 or scrambled siRNA treated cultures (** $P < 0.0005$ students T-test unpaired). (D) Longest neurite length of a single neuron of cultures treated with Mad1, or scrambled siRNA. All values were normalized to the scrambled values. (E) Number of branches per neurons normalized to the scrambled values ($N = 7$) (F) Immunohistochemistry staining for NF200 comparing the neurite outgrowth between the scrambled and Mad1 siRNA treated cultures.

4.3-2 Mad1 knockdown does not cause apoptosis in cultured DRG neurons

One concern to address was that although Myc regulates a variety of cellular growth pathways, overexpression of Myc can potentially cause apoptosis. To ensure that our Mad1 siRNA treatment was not sufficient to cause Myc dependent apoptosis, we performed a TUNEL analysis on cultures receiving Mad1 siRNA. This allowed us to examine apoptotic cells by observing if cells were TUNEL reactive, indicating there was DNA fragmentation, a feature of apoptosis. Following treatment and culture using the same timeline described in Figure 8A, we performed a TUNEL assay on DRG neuron cultures. We found that there was no significant difference between cells treated with Mad1 or scrambled siRNA (Figure 9).

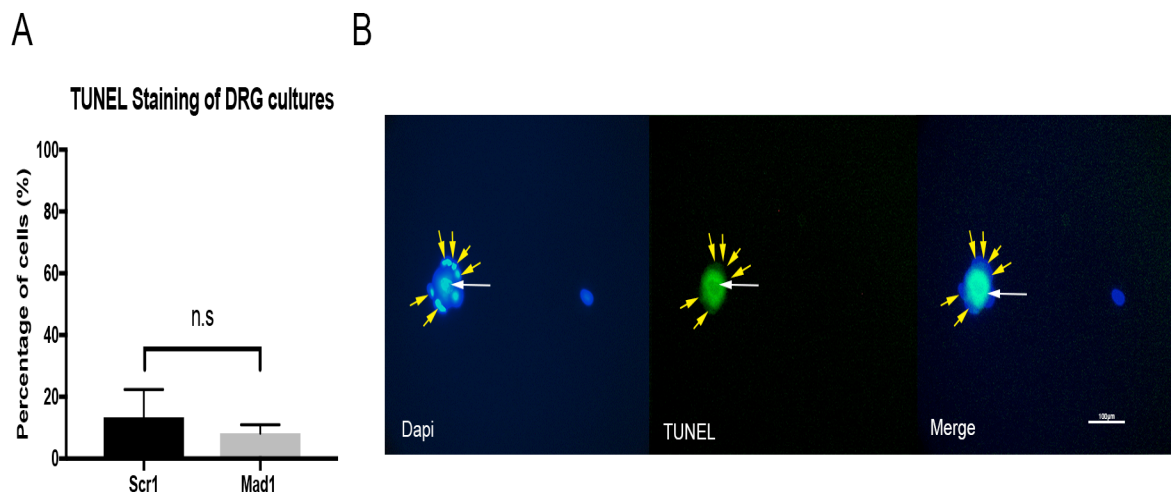


Figure 9: Mad1 knockdown does not increase apoptosis. (A) Quantification of percentage of apoptotic cells in media containing scrambled or Mad1 siRNA. (B) immunohistochemistry showing that the TUNEL assay was effective in staining DRG neurons. The yellow arrows show the perineuronal satellite cells and the white arrow indicates a TUNEL positive neuron. Bar=100µm

4.3-3 *c-Myc* Knockdown has no effect on neurite outgrowth

A similar experiment was performed using the timeline above (Figure 8A) with *c-Myc* siRNA. We found that upon treatment of these cultures with siRNA there was no significant decrease in the relative length of neurites, longest neurite or the number of neurons with sprouts (Figure 10). This finding appeared to contradict our original hypothesis that *c-Myc* knockdown should be associated with a reduction in overall sensory neurite growth. One possible explanation for the findings was that redundancy within the *Myc* family members may have allowed an alternate member to compensate for loss of *c-Myc*.

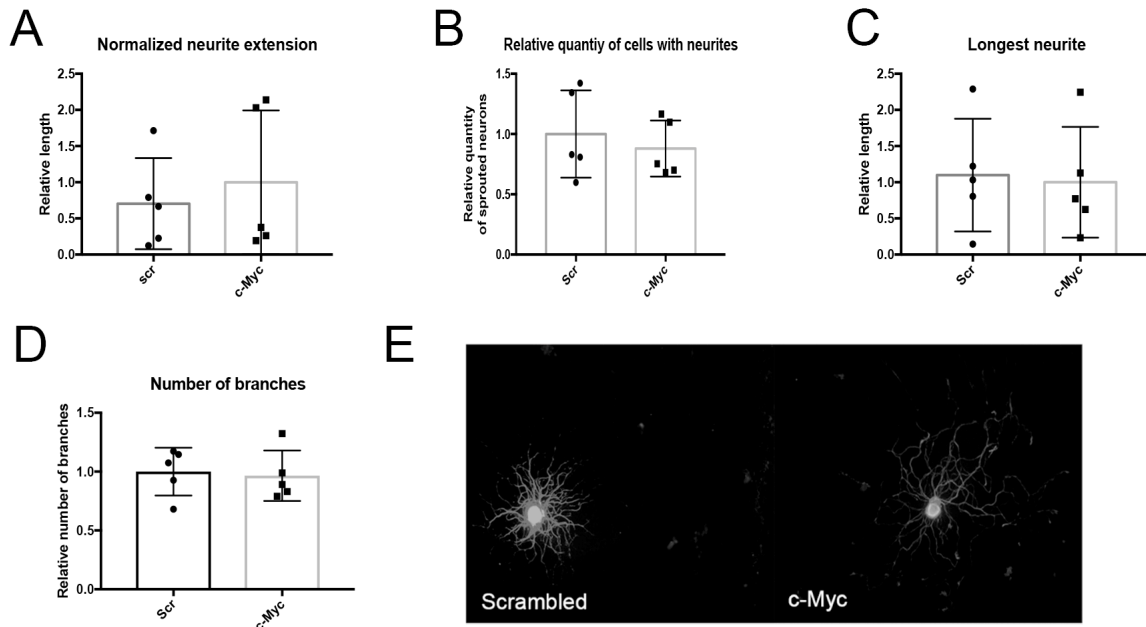


Figure 10: c-Myc knockdown does not alter neurite outgrowth. (A) The outgrowth of neurons cultured treated with 20nM c-Myc or scrambled sequence siRNA. All values were normalized to the scrambled sequence (N=5). (B) Percentage of neurons with sprouts compared to total population of neurons following treatment of c-Myc or scrambled siRNA. All values were normalized to scrambled values (N=5). (C) Longest neurites of a neuron in culture with c-Myc or scrambled siRNA, normalized to scrambled values (N=5). (D) Number of branches per neurons normalized to the scrambled values (N=5). (E) Immunohistochemistry showing similar levels of neurite outgrowth between the two treatment groups.

4.4 N-Myc expression, 10058-F4 and neurite outgrowth

4.4-1 N-Myc expression in injured and uninjured DRGs

We found that c-Myc knockdown in culture did not yield a reduction in DRG neuron regrowth, contrary to our hypothesis. We reasoned that this could be a result of compensation of other Myc proteins, more specifically N-Myc. qRT-PCR analysis of N-Myc at different time points following injury revealed that there are fluctuations in expression at 12, 36, and 72 hours (Figure 11). At 36 hours post injury, there is a significant decrease in the expression of N-Myc mRNA in the injured DRG compared to the uninjured control. There was a trend towards increased N-Myc expression at 72 hours post injury, similar to the pattern we see in c-Myc mRNA expression (Figure 3A). Therefore, we hypothesize that perhaps inhibition of both c, and N-Myc may be necessary to determine the importance of this pathway in the regenerating PNS.

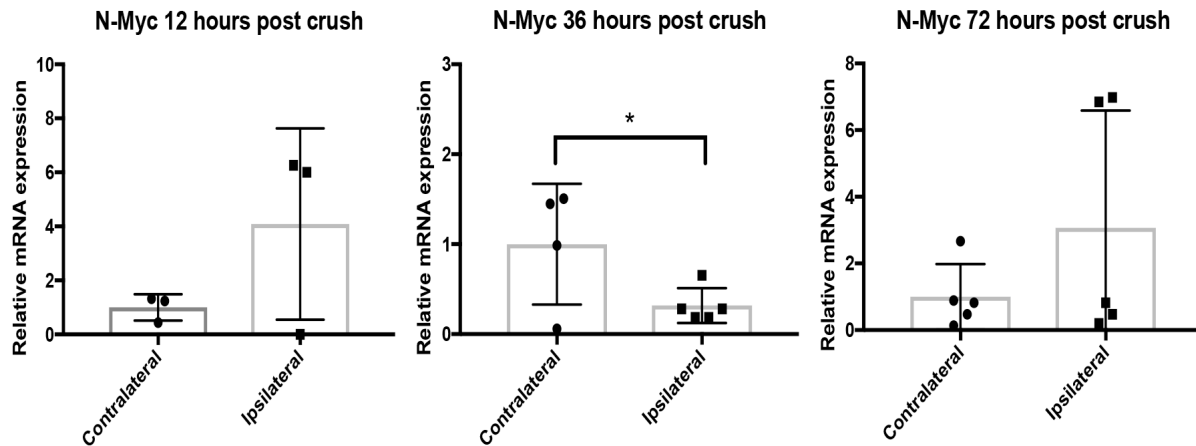


Figure 11: N-Myc expression is variable at different time points following sciatic nerve crush. qRT-PCR of N-Myc at 12, 36, and 72 hours normalized to the contralateral samples (12 hours n=3, 36 hours n=5, 72 hours n=5) (*P<0.05, students t test, N=5)

4.4-2 10058-F4 treated cultures decreases neurite outgrowth

Next, we tested whether if we inhibited the dimerization of Max with either N or c-Myc there would be an inhibitory effect on the neurite outgrowth *in vitro*. We used the specific Myc inhibitor 10058-F4 which has been shown to act on both of these Myc family members^{80,81}. We treated cultures with 6.4, or 64 uM 10058-F4. We found that treatment of cultures with 64uM 10058-F4 was capable of restricting neurite outgrowth with the lower dose trending towards significance (Figure 12A). The neurons cultured with 64uM 10058-F4 also showed a reduction in the percentage of neurons with neurites and also in the longest neurite compared to DMSO (carrier) treated controls (Figure 12B,C). The number of branches per neuron was reduced with both doses (Figure 12D). Figure E illustrates examples of of growth between DMSO and 10058-F4 treated neurons.

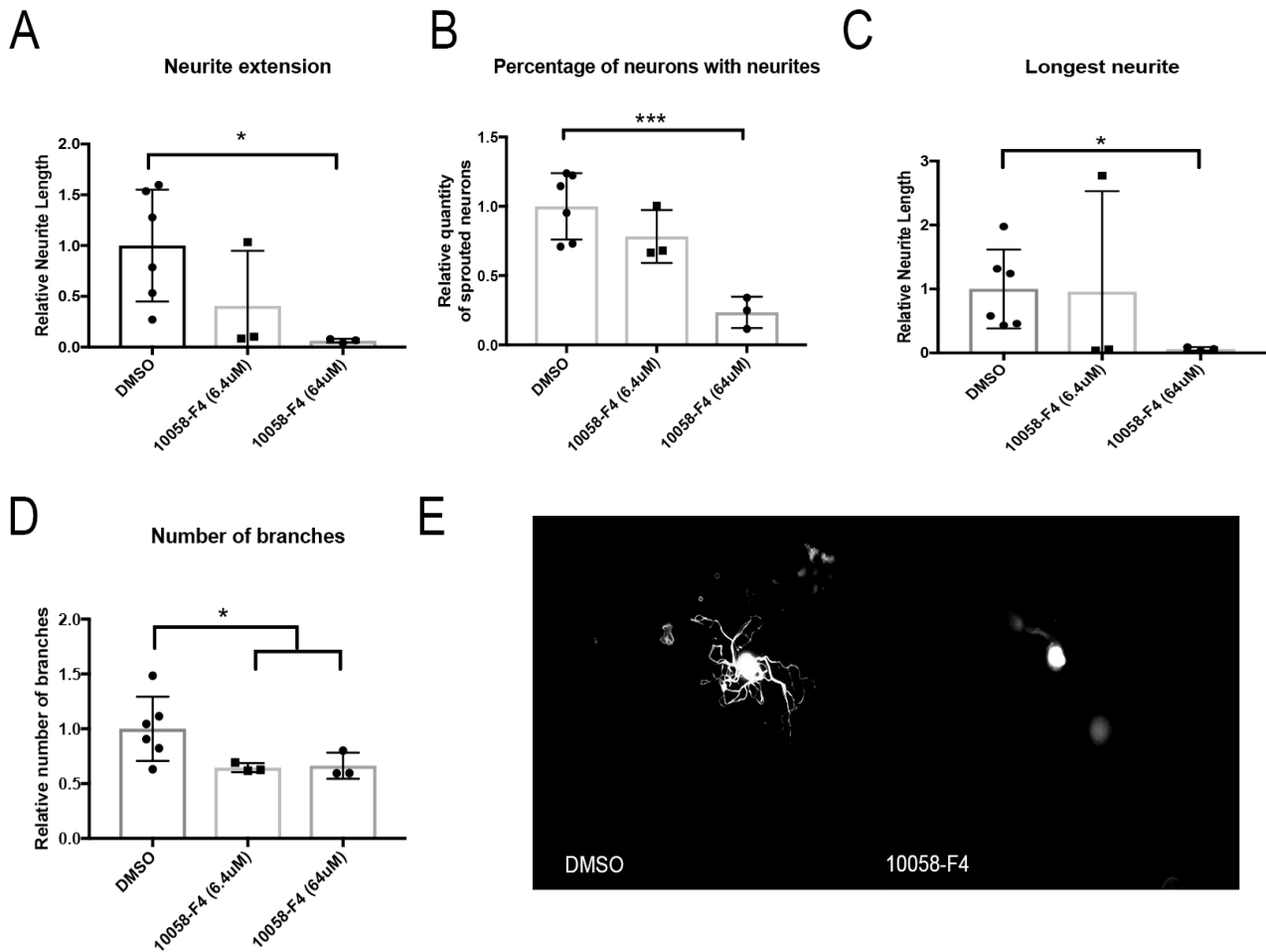


Figure 12: 10058-F4 treatment causes a reduction in the growth of DRG neurons *in vitro*. (A) The relative neurite extension of cultures treated with DMSO or 10058-F4 (6.4uM or 64uM). Values were normalized to DMSO values ($P^* < 0.05$, Students unpaired T Test, 10058-F4 n=3, DMSO n=6). (B) The percentage of neurons with neurites normalized to DMSO controls ($***P < 0.001$ Students unpaired T test 10058-F4 n=3, DMSO n=6). (C) longest neurite extension of a single neuron in cultures treated with 10058-F4 or DMSO. Values were normalized to DMSO controls ($P^* < 0.05$, Students unpaired T Test, 10058-F4 n=3, DMSO n=6). (D) Number of branches per neuron of either treatment conditions, normalized to DMSO treatment groups ($P^* < 0.05$, Students unpaired T Test, 10058-F4 n=3, DMSO n=6). (E) Images of cultures treated with 10058-F4 (64uM) or DMSO stained with NF200.

4.5 Mad1 siRNA *in vivo* experiments

Based on the improved neurite outgrowth associated with the knockdown of Mad1, we next moved our experiments into an *in vivo* model of nerve injury. In these experiments, mice had their baseline sensory tests including Hargreaves thermal sensitivity, Von Frey mechanical sensitivity, and multifiber nerve electrophysiology tested, before and following a high sciatic nerve crush injury. Animals then received 3 doses of siRNA delivered by local injection at the injury site with electroporation each week for 4 weeks. We repeated the above behavioral metrics again at 14 and 28 days. At 14 days, no sensory or motor compound action potentials were recordable in either group, as expected following a complete injury (not shown). At 28 days, we found that the sensory nerve action potentials (SNAP) had reappeared and their conduction velocities had dramatically improved to baseline levels. In contrast, there were severe and persistent reductions in the scrambled siRNA treated controls (Figure 13A). This improvement in velocity was only seen in the sensory axons and not in motor axons (Figure 13A, C). The amplitudes of both the sensory and the motor action potentials showed similar degrees of recovery, regardless of the treatment (Figure 13B, D). There was improvement in animals treated with Mad1 siRNA in withdrawal latency when presented with a thermal stimulus at 14 days post crush (Figure 13E). At 28 days, thermal sensitivity was similar between the groups. Animals treated with scrambled siRNA appear to be hypersensitive to the Von Frey filaments when compared to their Mad1 treated counterparts at both 14 and 28 days following injury (Figure 13F). In

contrast, mice treated with Mad1 siRNA had mechanical sensitivity that had recovered to baseline measurements. qRT-PCR analysis of Mad1 showed variability in knockdown of Mad1 following completion of the 28-day experiment (Figure 13G). Taken together, mice that had undergone Mad1 local siRNA administration had evidence of greater recovery in sensory electrophysiology and tests of sensory behavior than controls.

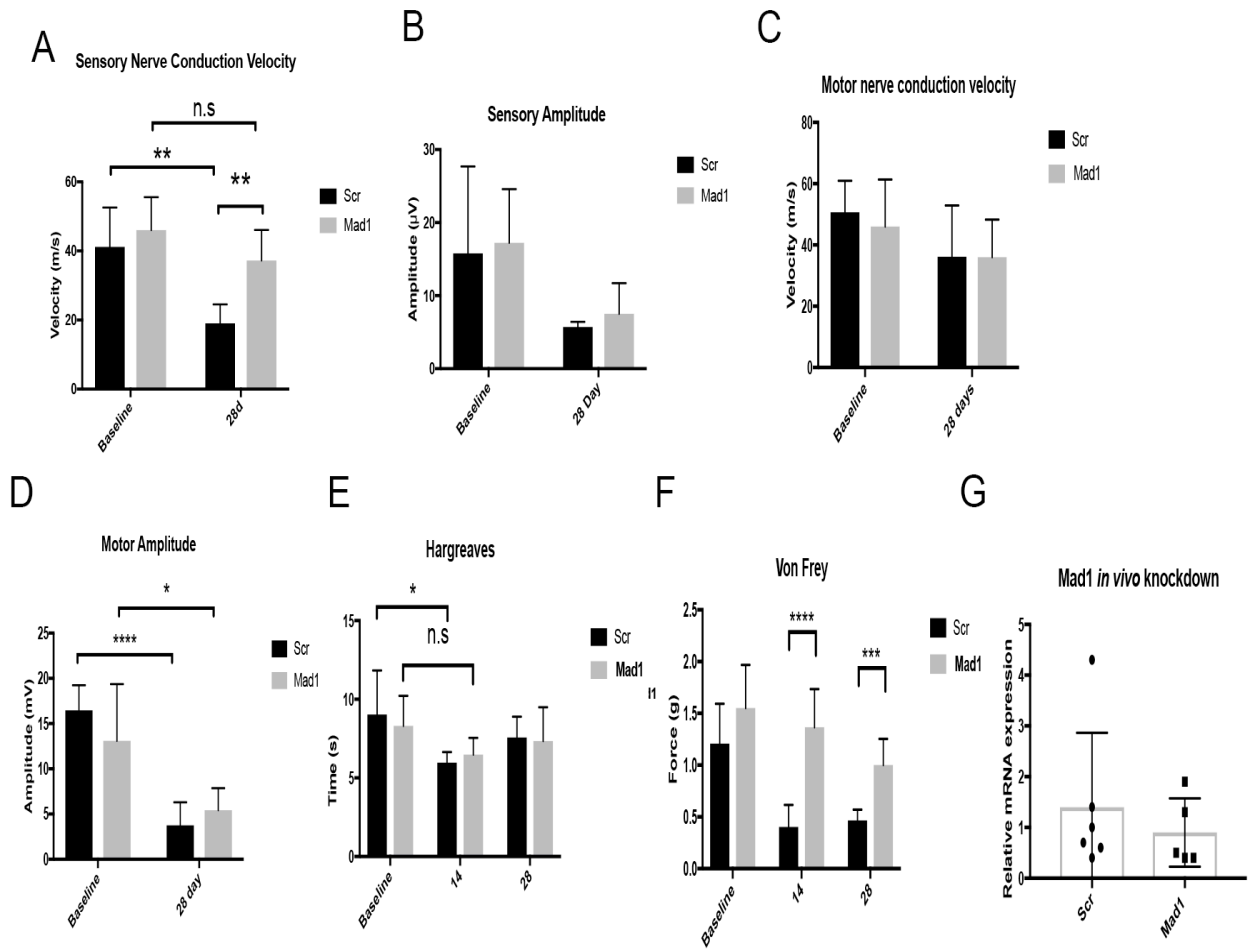


Figure 13: Mad1 siRNA treatments *in vivo* show improvements in behavioral and electrophysiological metrics post injury. (A) Sensory nerve conduction velocity of the sural nerve in animals treated with local injection and electroporation of Mad1 or scrambled siRNA. (**P<0.01 using student's unpaired T test n=6). (B) Amplitude of sensory nerve action potential of both Mad1 and scrambled treated animals(n=6). (C) Compound motor action potential (CMAP) velocity of the animals treated with either the Mad1 siRNA or scrambled sequence siRNA(n=6). (D) Average amplitude of motor compound muscle action potentials (CMAPs) measured at the sciatic notch and at the knee (****P<0.0001, *P<0.05 using student's unpaired T-test n=6). (E) Hargreaves thermal testing of withdrawal latencies of the ipsilateral hind paw in treatment groups (*P<0.05 using student's unpaired T test). (F) Von Frey testing measuring mechanical force required to elicit a withdrawal response in animals treated with either siRNA (****P<0.0001 ***P<0.0005 using student's unpaired t-test n=6). (G)qRT-PCR for Mad1 mRNA in animals treated with either scrambled or Mad1 siRNA.

5. Discussion

The present study evaluated the Myc/Mad/Max axis and the role that it plays in peripheral neurons and in their regeneration response. This is a novel pathway that has yet to be explored as a potential intervention point for amplifying the regrowth of axons following injury. We found that this important signaling axis was present within peripheral neurons. Furthermore, we could intervene and manipulate members of this pathway to cause growth enhancement of peripheral neurons. Regrowth of these neurons was also found to have behavioral implications, making this an exciting and novel pathway with implications on neuronal plasticity.

The data comparing the expression of these proteins was used to see if neurons normally react to damage through changes in these mediators. At the mRNA level, c-Myc was reduced 36 hours post injury and there were trends towards decreases in the mRNA of Max and Mad1 as well. This putative change was not observed in their protein concentrations but mRNA and protein levels can diverge. For example, other regulatory mechanisms may allow for increased stability, or mRNA changes may have been too small to account for overall changes in the protein pool. These findings confirmed evidence of neuron specific expression of the key players in this very potent growth signaling pathway, and is of considerable interest in examining neuron plasticity.

Additionally, there is the possibility that our time points for PCR may not have included earlier changes. Another consideration is that the expression of Myc Max and

Mad1 may have changed over a longer period of time and we did not test at these time points.

Phosphorylation of Myc plays a critical role in its stability⁵⁷. Possible differences in phosphorylated c-Myc at Ser 62 were not explored in this work but might identify evidence for its accumulation and stability, where it would promote growth and plasticity. Following injury, there could be changes in the accumulation of phosphorylated c-Myc and this may be indicative of the neurons being in a transmission or regenerative phenotype. For instance, if there were increased levels of c-Myc phosphorylation at threonine 58, there would be more degradation of c-Myc and this could be reflective of the neurons being in a quiescent state^{57,58}. Conversely, if there was enrichment of c-Myc phosphorylated on serine 62, the protein would be stabilized and perhaps this would be an indication that these neurons were in a state of growth and regeneration.

We explored Mad1's subcellular localization to the nucleolus within neurons to investigate if there is a difference in compartmentalization dependent on if the neurons are injured or not. We found Mad1 expression within the nucleolar compartment of the neurons, which has been previously described⁷⁹. It was found that Mad1 localized to the nucleolus had a suppressive effect on ribosomal biogenesis⁷⁹. We observed co-localization of Mad1 with fibrillarin, an rRNA o-methyltransferase specific to the nucleolus. We also explored whether Mad1 may show differences in nuclear/nucleolar localization in uninjured and injured DRGs. However, numbers of overall Mad1 positive nuclei were unchanged after injury. We did not explore injury-

related colocalization with a nucleolar marker, such as fibrillarin. Investigating the role Mad1 plays in ribosomal biosynthesis and how this influences PNS regeneration may prove to be interesting. It has been shown that ribosomes are transferred to regenerating axons by local SCs⁸². This is likely to aid in protein synthesis allowing elongation of the regenerating axon. In peripheral neurons it is uncertain whether Mad1-related alterations in ribosomal biosynthesis might play a role in regeneration. Since ongoing protein synthesis in perikarya and axons are essential to promote growth, this is an interesting function to consider. Similarly, there could potentially be a role for Mad1 in ribosomes transferred into axons from SCs, as described in other studies⁸².

The neurite outgrowth assay for this study has been very useful in providing metrics that we can use to quantify the degree of growth following a treatment. In order to determine what concentration of siRNA would cause significant knockdown, we used pooled cultures of DRG neurons from two rat DRG harvests to provide sufficient cells for PCR. Using the 20nM siRNA for either c-Myc or Mad1 in their respective cultures, was sufficient to cause knockdown of the associated transcripts, whereas paradoxically higher doses were unsuccessful in accomplishing this goal. Further experiments were then carried out with the 20nM dose.

Mad1 knockdown resulted in enhanced neurite extension and in total number of neurons that sprout *in vitro*. This presumably is through the elimination of Mad1's interaction with Max allowing Myc to function unhindered in these neurons. Myc's intense association with cell cycle mediators (Cyclins and CDKs) and growth related

proteins within all cell types, provide us with a preliminary basis to hypothesize the effect of Mad1 knockdown^{21,52}. We hypothesize that the increased plasticity of these neurons is a result of decreased competitive inhibition of Mad1 on the transcriptional functions of Myc. These striking results show a clear growth inhibitory role of Mad1 which has not been previously investigated within peripheral neurons.

While these findings were compelling, additional approaches to link neurite behaviour to elevated Myc gene transcription might include using a luciferase reporter gene, or a chromatin immunoprecipitation assay. These are examples of assays that might help link neurite extension to enhanced Myc signaling and can eliminate the possibility of an unknown function of these proteins. Despite these caveats, the current experiments act as a platform for future experiments that could further explore mechanism behind Mad1 within the peripheral nervous system. The findings confirm that substantial neuron plasticity can be effected in the setting of Mad1 knockdown.

The ability of Mad1 knockdown to increase the neurite length and the number of neurons with neurite sprouts in this experiment could be a product of NGF and the Myc pathway. Both the scrambled sequences and the Mad1siRNA treated cultures received NGF (100ng/ml) as part of the normal supportive media for adult sensory neurons, however the Mad1 siRNA treated cultures had greater neurite outgrowth. Physiological levels of NGF might activate the ERK1/2 signaling pathway and this has been linked to increased levels of stable phosphorylated Myc⁵⁷. With Myc phosphorylated and Mad1 knocked down by siRNA, there could be a synergistic effect of having both stable phospho-Myc and reduced Mad1 to inhibit Myc's effect.

Therefore, it is possible that the enhanced growth can be accounted for both of these cellular events.

Additionally, NGF can also activate PI3K signaling which involves downstream activation of Akt⁸³. Activation of this pathway can promote the formation of axon branches and filopodia projections of the growth cone that help it to sense its local environment^{6,83}. Earlier, we discussed the role that GSK3 β plays on Myc degradation and this can be counteracted by phosphorylation of GSK3 β by Akt on serine 9, whereas other kinases can activate GSK3 β by tyrosine 216 phosphorylation^{58,68}. Therefore it is possible that NGF stabilizes Myc through phosphorylation by ERK1/2 and preventing its degradation by inhibition of GSK3 β . This in collaboration with knockdown of Mad1 could contribute to the growth pattern we are seeing in the Mad1 knockdown cultures.

With the large array of genes that c-Myc regulates, observing changes within the proteome of neurons treated with Mad1 siRNA might be informative to determine mechanisms for this enhancement of outgrowth. Such approaches could include two dimensional liquid chromatography-tandem mass spectrometry (2D-LC-MS/MS), of cultures treated with Mad1 siRNA. This would help to identify candidate proteins that we could further investigate as playing a role in the regrowth mechanism.

Over activity of Myc genes can cause apoptosis, however in the present study we found no increase in the TUNEL reactivity of cells following Mad1 siRNA administration^{17,21,53}. This assay labels fragmented DNA, a feature of apoptosis and will conjugate a detectable molecule onto these fragments which can be visualized using fluorescent microscopy. There have been previous studies that show that dysregulation

of Myc is not capable of driving apoptosis, but rather primes the apoptotic machinery and upon administration of another insult, will cause an exaggerated apoptotic response⁵⁵. We speculated that perhaps the sensory axotomy along with Mad1 knockdown, and subsequent Myc dysregulation could cause enhanced apoptosis of our cultured neurons. However our TUNEL assay results showed that this was not the case. Furthermore, the morphology of the DRG neurons in culture appeared to be normal and did not indicate that there was apoptosis. These neurons did not show apoptotic blebbing and these neurons appear to be uniform indicating they were not in a state of programmed cell death. Although our TUNEL assays were done *in vitro*, our *in vivo* siRNA treated animals may show a different pattern, but we think this is unlikely since they demonstrated improved sensory behaviour.

The c-Myc treated cultures revealed a different result than expected. We reasoned that if we knocked down c-Myc, this would cause a reduction in neurite extension. However, this did not prove to be the case. One important way to explain this is that there are other Myc family members that could be compensating for the loss of c-Myc. N-Myc is also a prominent transcription factor that when conditionally knocked out during development, shows a greater growth reduction in brain mass than c-Myc⁵⁰. With emphasis on c-Myc in cancer literature, we chose this protein as our primary target but N-Myc may be also important within the nervous system. N-Myc can also be oncogenic and has been associated with retinoblastoma tumours similar to RB1 mutations. It is therefore likely that N-Myc can impact the growth and transformation of normal cells as well²⁰. For this reason, we cultured adult DRG

neurons in the presence of a small molecule inhibitor 10058-F4 which has been shown to inhibit both c-Myc and N-Myc dimerization with Max^{80,81}. This small molecule is capable of perturbing the interaction of the bHLH domains of Myc and Max and therefore, can inhibit their transcriptional effects⁸⁰. 10058-F4 has been evaluated within models of cancer for its ability to reduce the Myc-Max interaction and abrogate tumour cell growth^{84,85}

We observed N-Myc expression at varying times post injury. There were similar fluctuations in expression compared to the expression patterns of c-Myc. We therefore decided to examine a generalized but specific inhibitor of c-Myc and N-Myc, 10058-F4. In dissociated adult sensory neurons exposed to 64uM 10058-F4 we noted a substantial reduction in total neurite extension, the number of branches per neuron, longest neurite and the percentage of neurons with sprouts compared to DMSO controls. For our *in vitro* experiments, we used 64uM 10058-F4 which has shown to be effective in preventing cell division^{80,81}. We also used a lower dose (6.4uM) and found that there were trends towards significance in all of the above metrics. Future work could consider additional dose ranging and assessment of the apoptosis profiles of these cultures. Our cultures containing 10058-F4 showed a nonsignificant trend toward reduction in cell number compared to DMSO controls (data not shown), indicating that assessment of cell survival of these neurons may be an important consideration.

Our Mad1 *in vivo* studies identified impacts on sensory function of regenerating nerves. We observed an enhancement in sensory nerve conduction velocity in the animals treated with the Mad1 siRNA. This may be a result of greater

radial growth and maturation of regenerating axons or could also be explained by a non-specific knockdown of the Mad1 gene in the surrounding SC population. Enhanced myelination of the regenerating axons could contribute to improvements in the sensory nerve conduction. However, we do not see improvements within the motor nerve conduction velocity.

There were also impacts on the recovery of mechanical and thermal sensibility after injury. The Hargreaves showed an improvement in thermal sensitivity at 14 days whereas the scrambled treated controls did not. Additionally, the Von Frey mechanical testing did show a marked improvement in these animals when testing mechanical allodynia. The scrambled treated animals were hypersensitive to the Von Frey filaments and improved slightly at 28 days. This hypersensitivity following crush surgeries has been shown in other studies⁸⁶. Since the mice receiving Mad1 siRNA showed return of sensitivity to baseline at 14 days the sensitivity of these animals to painful mechanical stimuli may have also been altered by our approach.

In our *in vivo* experiments we used local injection and electroporation to administer our siRNA treatments. Previous studies have shown that siRNA can be retrogradely transported to the DRG and can cause reduction in associated protein or mRNA expression^{22,29}. Furthermore, we used local electroporation to increase the permeability of the axons to augment siRNA uptake. Our qRT-PCR data show that there was a nonsignificant trend toward decreased Mad1 mRNA expression following treatment with Mad1 siRNA. Since these measures do suffer from inherent variability, additional studies to confirm knockdown will be needed. The mice received siRNA 3

days a week for 28 days, it is possible that over the course of the experiments the neurons compensated for the decrease in mRNA induced by the siRNA to try to normalize levels of Mad1 or clear siRNA more quickly over time. In future experiments important steps will be to probe for changes in the levels of Mad1 protein following siRNA treatments, or look at the mRNA expression at 7 days and determine whether within early time points there is significant knockdown. Furthermore, we locally injected and electroporated at the crush site, so there could have potentially been significant knockdown in SCs in the area, a possibility, mentioned above worth exploring.

In this thesis, we have primarily investigated the contribution of Mad1 and c-Myc on the plasticity of regenerating neurons. Although there is enhanced growth in Mad1 knocked down neurons, *in vivo* there could also be a response of the SCs. Neurons are not expected to divide, but following an injury to the nerve the SCs rapidly proliferate and help facilitate regeneration. In regenerating microenvironments, the very close collaboration of growing axons and their SCs can make it difficult to tease out the importance of each player. Mad1 knockdown could also influence the proliferation and divisional capabilities in SCs. Additionally, SCs that have knockdown of Mad1 could have augmented division and this could potentially promote more rapid axonal degeneration of the distal segment, clearing the way for newly regenerating axons.

Electron microscopy is a helpful tool that examines morphological changes in myelination and organization such as the g-ratio of the myelinated axons after injury.

This approach would identify changes in the myelin thickness around these axons associated with altered SC behaviour.

Another possibility is that the SCs could be providing additional mitogenic, and neurotrophic support to the regenerating axons. SCs have been shown to release a variety of regeneration supportive molecules including growth factors, adhesion molecules, and guidance cues for new axons^{6,87}. Experimentally, changes in supportive and growth enhancing molecules released by SCs could be identified by culturing SCs in media containing Mad1 or scrambled siRNA, and then by growing DRG neurons in the conditioned media. This would allow for us to observe if the SCs exposed to Mad1 siRNA are better at supporting neurite outgrowth.

Max is a central player within this signaling axis. It has been shown to be mutated in a subset of pheochromocytoma patients⁷⁴. Here we did not evaluate the effect of Max knockdown. It has been speculated that Max may play more of a repressive role within this network, as dysfunction of this protein can cause cancer^{73,74}. It is conceivable that knock down of Max could enhance the regeneration of axons in similar fashion to Mad1.

Overall our experiments characterizing expression and role of members of the Myc/Mad1/Max signaling axis have identified novel molecules governing neuronal plasticity. Expression of these mediators does not change intrinsically following injury to coordinate the regrowth of axons. However, through the use of siRNA we have demonstrated the role of Myc and Mad1 in the regenerative response. Mad1 knockdown is capable of driving enhanced neurite outgrowth *in vitro* and additionally

can improve the sensory behavior of mice in our sciatic crush model of nerve injury. These findings provide an exciting foundation for further research into the mechanistic function of Mad1 and add it to the list of mediators affecting the growth capabilities of neurons.

The Myc oncogene, although extensively studied in cancer, has not been evaluated in the PNS as an intervention point for influencing the plasticity of damaged nerves. Here we show that c-Myc is not critical for the regeneration response *in vitro* through our siRNA treated cultures. Although, our small molecule inhibitor of both N and c-Myc show that these proteins are essential for permitting the growth of damaged sensory neurons. These results illustrate the importance of this family of essential growth permitting molecules. Determining the mechanism of novel proteins like Mad1 and c-Myc in the peripheral nervous system provide an important basis for drug discovery for therapeutic agents that augment the recovery of patients suffering from nerve injury or neuropathy.

Conclusion

This thesis outlined the expression of Myc, Mad1 and Max within the DRG and investigated the effect that these molecules have on regrowth of axons following injury. Mad1 knockdown was capable of improving *in vitro* and *in vivo* regeneration of peripheral neurons. 10058-F4 inhibition of N and c-Myc was able to dampen the regeneration response of DRG neurons *in vivo*. Mad1 joins the list of mediators that play a role in the plasticity of regenerating neurons and this work can be used as a foundation for further investigation into its growth promoting role.

References

1. Kusano, K. *et al.* Enhancement of sciatic nerve regeneration by adenovirus-mediated expression of dominant negative RhoA and Rac1. *Neurosci. Lett.* **492**, 64–69 (2011).
2. Christie, K. J., Webber, C. A., Martinez, J. A., Singh, B. & Zochodne, D. W. PTEN Inhibition to Facilitate Intrinsic Regenerative Outgrowth of Adult Peripheral Axons. *J. Neurosci.* **30**, 9306–9315 (2010).
3. Christie, K. J. *et al.* Enhancing adult nerve regeneration through the knockdown of retinoblastoma protein. *Nat Commun* **5**, 3670 (2014).
4. Krishnan, A., Duraikannu, A. & Zochodne, D. W. Releasing ‘brakes’ to nerve regeneration: Intrinsic molecular targets. *European Journal of Neuroscience* **43**, 297–308 (2016).
5. Witzel, C., Rohde, C. & Brushart, T. M. Pathway sampling by regenerating peripheral axons. *J. Comp. Neurol.* **485**, 183–190 (2005).
6. Zochodne, D. W. *Neurobiology of Peripheral Nerve Regeneration*. (Cambridge, 2008).
7. Zochodne, D. W. The challenges and beauty of peripheral nerve regrowth. in *Journal of the Peripheral Nervous System* **17**, 1–18 (2012).
8. Van Der Veen, R. C. & Roberts, L. J. Contrasting roles for nitric oxide and peroxynitrite in the peroxidation of myelin lipids. *J. Neuroimmunol.* **95**, 1–7 (1999).
9. Li, R. *et al.* Peripheral Nerve Injuries Treatment: A Systematic Review. *Cell Biochemistry and Biophysics* **68**, 449–454 (2014).
10. Huang, J., Zhang, Y., Lu, L., Hu, X. & Luo, Z. Electrical stimulation accelerates

- nerve regeneration and functional recovery in delayed peripheral nerve injury in rats. *Eur. J. Neurosci.* **38**, 3691–701 (2013).
11. Al-Majed, A. a, Neumann, C. M., Brushart, T. M. & Gordon, T. Brief electrical stimulation promotes the speed and accuracy of motor axonal regeneration. *J. Neurosci.* **20**, 2602–2608 (2000).
 12. Archibald, S. J., Shefner, J., Krarup, C. & Madison, R. D. Monkey median nerve repaired by nerve graft or collagen nerve guide tube. *J. Neurosci.* **15**, 4109–4123 (1995).
 13. Guénard, V., Kleitman, N., Morrissey, T. K., Bunge, R. P. & Aebischer, P. Syngeneic Schwann cells derived from adult nerves seeded in semipermeable guidance channels enhance peripheral nerve regeneration. *J. Neurosci.* **12**, 3310–3320 (1992).
 14. Neal, R. A. *et al.* Alignment and composition of laminin-polycaprolactone nanofiber blends enhance peripheral nerve regeneration. *J. Biomed. Mater. Res. - Part A* **100 A**, 406–423 (2012).
 15. Indovina, P., Pentimalli, F., Casini, N., Vocca, I. & Giordano, A. RB1 dual role in proliferation and apoptosis: cell fate control and implications for cancer therapy. *Oncotarget* **6**, 17873–90 (2015).
 16. Adlkofer, K. *et al.* Hypermyelination and demyelinating peripheral neuropathy in Pmp22-deficient mice. *Nat. Genet.* **11**, 274–280 (1995).
 17. Oster, S. K., Ho, C. S. W., Soucie, E. L. & Penn, L. Z. The myc oncogene: Marvelously complex. *Advances in Cancer Research* **84**, 81–154 (2002).

18. Johnston, L. a, Prober, D. a, Edgar, B. a, Eisenman, R. N. & Gallant, P. *Drosophila myc* regulates cellular growth during development. *Cell* **98**, 779–90 (1999).
19. Ladu, S. *et al.* E2F1 Inhibits c-Myc-Driven Apoptosis via PIK3CA/ Akt/mTOR and COX-2 in a Mouse Model of Human Liver Cancer. *Gastroenterology* **135**, 1322–1332 (2008).
20. Rushlow, D. E. *et al.* Characterisation of retinoblastomas without RB1 mutations: Genomic, gene expression, and clinical studies. *Lancet Oncol.* **14**, 327–334 (2013).
21. Dang, C. V. *et al.* The c-Myc target gene network. *Seminars in Cancer Biology* **16**, 253–264 (2006).
22. Singh, B. *et al.* Regeneration of diabetic axons is enhanced by selective knockdown of the PTEN gene. *Brain* **137**, 1051–1067 (2014).
23. Hu, G. *et al.* Single-cell RNA-seq reveals distinct injury responses in different types of DRG sensory neurons. *Sci. Rep.* **6**, (2016).
24. Gey, M. *et al.* Atf3 mutant mice show reduced axon regeneration and impaired regeneration-associated gene induction after peripheral nerve injury. *Open Biol.* **6**, 53–53 (2016).
25. Ying, Z., Misra, V. & Verge, V. M. K. Sensing nerve injury at the axonal ER: Activated Luman/CREB3 serves as a novel axonally synthesized retrograde regeneration signal. *Proc. Natl. Acad. Sci.* **111**, 16142–16147 (2014).
26. Richardson, P. M. & Issa, V. M. K. Peripheral injury enhances central regeneration of primary sensory neurones. *Nature* **309**, 791–793 (1984).
27. Nie, Z. *et al.* c-Myc Is a Universal Amplifier of Expressed Genes in Lymphocytes

- and Embryonic Stem Cells. *Cell* **151**, 68–79 (2012).
28. Kennedy, J. M. & Zochodne, D. W. Impaired peripheral nerve regeneration in diabetes mellitus. *J. Peripher. Nerv. Syst.* **10**, 144–57 (2005).
 29. Webber, C. A. *et al.* Schwann cells direct peripheral nerve regeneration through the Netrin-1 receptors, DCC and Unc5H2. *Glia* **59**, 1503–1517 (2011).
 30. Toth, C. C. *et al.* Locally synthesized calcitonin gene-related peptide has a critical role in peripheral nerve regeneration. *J. Neuropathol. Exp. Neurol.* **68**, 326–337 (2009).
 31. Clements, M. P. *et al.* The Wound Microenvironment Reprograms Schwann Cells to Invasive Mesenchymal-like Cells to Drive Peripheral Nerve Regeneration. *Neuron* **96**, 98–114.e7 (2017).
 32. Triolo, D. Loss of glial fibrillary acidic protein (GFAP) impairs Schwann cell proliferation and delays nerve regeneration after damage. *J. Cell Sci.* **119**, 3981–3993 (2006).
 33. Smith, K. N., Lim, J. M., Wells, L. & Dalton, S. Myc orchestrates a regulatory network required for the establishment and maintenance of pluripotency. *Cell Cycle* **10**, 592–597 (2011).
 34. Cartwright, P. LIF/STAT3 controls ES cell self-renewal and pluripotency by a Myc-dependent mechanism. *Development* **132**, 885–896 (2005).
 35. Okita, K., Ichisaka, T. & Yamanaka, S. Generation of germline-competent induced pluripotent stem cells. *Nature* **448**, 313–317 (2007).
 36. Belin, S. *et al.* Injury-Induced Decline of Intrinsic Regenerative Ability Revealed

- by Quantitative Proteomics. *Neuron* **86**, 1000–1014 (2015).
37. Sheiness, D., Fanshier, L. & Bishop, J. M. Identification of nucleotide sequences which may encode the oncogenic capacity of avian retrovirus MC29. *J. Virol.* **28**, 600–10 (1978).
 38. Nilsson, J. a & Cleveland, J. L. Myc pathways provoking cell suicide and cancer. *Oncogene* **22**, 9007–9021 (2003).
 39. Kohl, N. E. *et al.* Transposition and amplification of oncogene-related sequences in human neuroblastomas. *Cell* **35**, 359–367 (1983).
 40. Nau, M. M. *et al.* L-myc, a new myc-related gene amplified and expressed in human small cell lung cancer. *Nature* **318**, 69–73 (1985).
 41. Beltran, H. The N-myc Oncogene: Maximizing its Targets, Regulation, and Therapeutic Potential. *Mol. Cancer Res.* **12**, 815–822 (2014).
 42. Niu, Z. *et al.* Knockdown of c-Myc inhibits cell proliferation by negatively regulating the Cdk/Rb/E2F pathway in nasopharyngeal carcinoma cells. *Acta Biochim. Biophys. Sin. (Shanghai)*. **47**, 183–191 (2015).
 43. Kim, S., Li, Q., Dang, C. V & Lee, L. a. Induction of ribosomal genes and hepatocyte hypertrophy by adenovirus-mediated expression of c-Myc in vivo. *Proc. Natl. Acad. Sci. U. S. A.* **97**, 11198–11202 (2000).
 44. James, L. & Eisenman, R. N. Myc and Mad bHLHZ domains possess identical DNA-binding specificities but only partially overlapping functions in vivo. *Proc. Natl. Acad. Sci. U. S. A.* **99**, 10429–34 (2002).
 45. Foley, K. P. *et al.* Targeted disruption of the MYC antagonist MAD1 inhibits cell

- cycle exit during granulocyte differentiation. *EMBO J.* **17**, 774–785 (1998).
46. Raffeiner, P. *et al.* In vivo quantification and perturbation of Myc-Max interactions and the impact on oncogenic potential. *Oncotarget* **5**, 8869–8878 (2014).
 47. Yang, J. *et al.* The role of histone demethylase KDM4B in Myc signaling in neuroblastoma. *J. Natl. Cancer Inst.* **107**, (2015).
 48. Magri, L. *et al.* C-Myc-dependent transcriptional regulation of cell cycle and nucleosomal histones during oligodendrocyte differentiation. *Neuroscience* **276**, 72–86 (2014).
 49. Han, S. M., Baig, H. S. & Hammarlund, M. Mitochondria Localize to Injured Axons to Support Regeneration. *Neuron* **92**, 1308–1323 (2016).
 50. Wey, A., Cerdeno, V. M., Pleasure, D. & Knoepfler, P. S. c- and N-myc regulate neural precursor cell fate, cell cycle, and metabolism to direct cerebellar development. *Cerebellum* **9**, 537–547 (2010).
 51. Cavalheiro, G. R., Matos-Rodrigues, G. E., Gomes, A. L., Rodrigues, P. M. G. & Martins, R. A. P. c-myc regulates cell proliferation during lens development. *PLoS One* **9**, (2014).
 52. Bretones, G., Delgado, M. D. & León, J. Myc and cell cycle control. *Biochimica et biophysica acta* **1849**, 506–516 (2015).
 53. Mitchell, K. O. *et al.* Bax is a transcriptional target and mediator of c-Myc-induced apoptosis. *Cancer Res.* **60**, 6318–6325 (2000).
 54. Askew, D. S., Ashmun, R. A., Simmons, B. C. & Cleveland, J. L. Constitutive c-

- myc expression in an IL-3-dependent myeloid cell line suppresses cell cycle arrest and accelerates apoptosis. *Oncogene* **6**, 1915–22 (1991).
55. Murphy, D. J. *et al.* Distinct Thresholds Govern Myc's Biological Output In Vivo. *Cancer Cell* **14**, 447–457 (2008).
 56. Szklarczyk, D. *et al.* STRING v10: Protein-protein interaction networks, integrated over the tree of life. *Nucleic Acids Res.* **43**, D447–D452 (2015).
 57. Sears, R. *et al.* Multiple Ras-dependent phosphorylation pathways regulate Myc protein stability. *Genes Dev.* **14**, 2501–2514 (2000).
 58. Knoepfler, P. S. & Kenney, A. M. Neural precursor cycling at sonic speed: N-Myc pedals, GSK-3 brakes. *Cell Cycle* **5**, 47–52 (2006).
 59. Guo, X., Snider, W. D. & Chen, B. Gsk3?? regulates AKT-induced central nervous system axon regeneration via an eIF2B?? -dependent, mTORC1-independent pathway. *Elife* **5**, (2016).
 60. He, T. C. *et al.* Identification of c-MYC as a target of the APC pathway. *Science* (80-.). **281**, 1509–1512 (1998).
 61. Duraikannu, A., Krishnan, A. & Zochodne, D. W. EXPANDING THE REPERTOIRE OF TUMOUR MOLECULES IN NEURONS: THE CASE FOR APC, beta-CATENIN SIGNALLING AND REGENERATION. *Soc. Neurosci.* (2016).
 62. Jin, Z., May, W. S., Gao, F., Flagg, T. & Deng, X. Bcl2 suppresses DNA repair by enhancing c-Myc transcriptional activity. *J. Biol. Chem.* **281**, 14446–14456 (2006).
 63. Chiarugi, V. & Ruggiero, M. Role of three cancer 'master genes' p53, bcl2 and c-myc on the apoptotic process. *Tumori* **82**, 205–209 (1996).

64. Cheng, N. *et al.* Bcl-2 inhibition of T-cell proliferation is related to prolonged T-cell survival. *Oncogene* **23**, 3770–3780 (2004).
65. Wang, Z.-M., Dai, C.-F., Kanoh, N., Chi, F.-L. & Li, K.-Y. Apoptosis and expression of BCL-2 in facial motoneurons after facial nerve injury. *Otol. Neurotol.* **23**, 397–404 (2002).
66. Marampon, F., Ciccarelli, C. & Zani, B. M. Down-regulation of c-Myc following MEK/ERK inhibition halts the expression of malignant phenotype in rhabdomyosarcoma and in non muscle-derived human tumors. *Mol. Cancer* **5**, (2006).
67. Wuhanqimuge, Itakura, A., Matsuki, Y., Tanaka, M. & Arioka, M. Lysophosphatidylcholine enhances NGF-induced MAPK and Akt signals through the extracellular domain of TrkA in PC12 cells. *FEBS Open Bio* **3**, 243–251 (2013).
68. Medina, M. & Wandosell, F. Deconstructing GSK-3: The Fine Regulation of Its Activity. *Int. J. Alzheimers. Dis.* **2011**, 1–12 (2011).
69. Lüscher, B. MAD1 and its life as a MYC antagonist: An update. *European Journal of Cell Biology* **91**, 506–514 (2012).
70. Quéva, C., Hurlin, P. J., Foley, K. P. & Eisenman, R. N. Sequential expression of the MAD family of transcriptional repressors during differentiation and development. *Oncogene* **16**, 967–77 (1998).
71. Coppola, J. A. & Cole, M. D. Constitutive c-myc oncogene expression blocks mouse erythroleukaemia cell differentiation but not commitment. *Nature* **320**, 760–763 (1986).

72. Foley, K. P. & Eisenman, R. N. Two MAD tails: What the recent knockouts of Mad1 and Mxi1 tell us about the MYC/MAX/MAD network. *Biochimica et Biophysica Acta - Reviews on Cancer* **1423**, (1999).
73. Cascoñ, A. & Robledo, M. MAX and MYC: A heritable breakup. *Cancer Research* **72**, 3119–3124 (2012).
74. Comino-Méndez, I. *et al.* Exome sequencing identifies MAX mutations as a cause of hereditary pheochromocytoma. in *Nature Genetics* **43**, 663–667 (2011).
75. Ribon, V., Leff, T. & Saltiel, A. R. C-Myc does not require Max for transcriptional activity in PC-12 cells. *Mol. Cell. Neurosci.* **5**, 277–282 (1994).
76. Gallant, P. & Steiger, D. Myc's secret life without Max. *Cell Cycle* **8**, 3848–3853 (2009).
77. Rishal, I. *et al.* WIS-neuromath enables versatile high throughput analyses of neuronal processes. *Dev. Neurobiol.* **73**, 247–256 (2013).
78. Hargreaves, K., Dubner, R., Brown, F., Flores, C. & Joris, J. A new and sensitive method for measuring thermal nociception in cutaneous hyperalgesia. *Pain* **32**, 77–88 (1988).
79. Lafita-Navarro, M. C. *et al.* MXD1 localizes in the nucleolus, binds UBF and impairs rRNA synthesis. *Oncotarget* (2016). doi:10.18632/oncotarget.11766
80. Yin, X., Giap, C., Lazo, J. S. & Prochownik, E. V. Low molecular weight inhibitors of Myc-Max interaction and function. *Oncogene* **22**, 6151–6159 (2003).
81. Müller, I. *et al.* Targeting of the MYCN protein with small molecule c-MYC inhibitors. *PLoS One* **9**, (2014).

82. Court, F. A. *et al.* Morphological evidence for a transport of ribosomes from Schwann cells to regenerating axons. *Glia* **59**, 1529–1539 (2011).
83. Ketschek, A. & Gallo, G. Nerve Growth Factor Induces Axonal Filopodia through Localized Microdomains of Phosphoinositide 3-Kinase Activity That Drive the Formation of Cytoskeletal Precursors to Filopodia. *J. Neurosci.* **30**, 12185–12197 (2010).
84. Huang, M. J., Cheng, Y. chih, Liu, C. R., Lin, S. & Liu, H. E. A small-molecule c-Myc inhibitor, 10058-F4, induces cell-cycle arrest, apoptosis, and myeloid differentiation of human acute myeloid leukemia. *Exp. Hematol.* **34**, 1480–1489 (2006).
85. Wang, J. *et al.* Evaluation of the antitumor effects of c-Myc-Max heterodimerization inhibitor 100258-F4 in ovarian cancer cells. *J. Transl. Med.* **12**, (2014).
86. Poplawski, G. *et al.* Schwann cells regulate sensory neuron gene expression before and after peripheral nerve injury. *Glia* **1**, 1–14 (2018).
87. Webber, C. & Zochodne, D. The nerve regenerative microenvironment: Early behavior and partnership of axons and Schwann cells. *Experimental Neurology* **223**, 51–59 (2010).